A Model-based Calibration Method for the Design of Wearable and Cuffless Devices Measuring Arterial Blood Pressure

LIU, Yinbo

A Thesis Submitted in Partial Fulfillment

of the Requirements for the Degree of

Master of Philosophy

in

Electronic Engineering

September 2008

Abstract

The monitoring of blood pressure (BP) is vitally important regarding the strikingly increasing number of hypertensives and the severe consequences of high blood pressure which has no symptom. Over the past several decades, a pulse transit time (PTT)-based technique has drawn a lot of interests as it provides a potential way to estimate blood pressure (BP) noninvasivly and continuously. Nonetheless, the relationship between BP and PTT varied from subject to subject and thus a major challenge of the PTT-based method is to calibrate it individually in a simple and accurate way. Most of the conventional calibration methods involve complicated procedures or multiple BP readings from cuff-based devices, which makes the calibration approach inconvenient.

Therefore, the objective of this study is to investigate factors e.g. dynamic exercise, external cuff pressure and hydrostatic pressure that could induce changes in BP and/or PTT to develop a calibration method for BP estimation.

Three experiments that induced whole body or local pressure changes were conducted. Experiment 1 involved a whole-arm elevation test. Experiment 2 was conducted in a dynamic exercise session. Experiment 3 introduced external force that was applied on the brachial artery. Based on the results of these experiments, we developed a model describing the relationship between PTT and finger height during arm elevation. Through this procedure, coefficients that are subject to individuals could be calibrated.

An experiment including 28 subjects was carried out to verify this hydrostatic calibration approach. This test was composed of a calibration session with arm elevation and an estimation session which included resting and post-exercise conditions. The results of this test showed that: 1) by using two PTT values at different heights and the arm length of a subject, this approach can calculate the

changes in his/her BP in a totally cuffless manner and 2) using two PTTs and one BP value measured under resting condition, this approach can obtain an overall systolic blood pressure estimation error of -2.8±7.7 mmHg.

The results of this study show that the potential of using the hydrostatic calibration method for BP monitoring and monitoring changes of BP without using any cuff-based device.

论文摘要

高血压是一种被称为“无声的杀手”的疾病，它无痛无创却能引起一系列严重的连带疾病并破坏人体的重要器官。随着患者数目的激增，致病原因的多样化以及受众范围的扩大，对人体血压的监测在当前医疗保健日益受到重视的发展趋势下的显得尤为重要。在过去的几十年中，一种新型的基于脉搏波传输时间的技术为非侵入式连续血压测量提供了可行的方法，从而引起了人们的兴趣和重视。然而，由于每个个体自身的血压和脉搏波传输时间之间的关系存在着差异，在估测模型中将有一些个人特征系数需要预先计算来获取（校准）。现有的校准方法多需用到复杂的仪器及步骤，或者需要从袖带式血压计读取多次血压值，不仅让校准过程变得繁冗不便，也增加了设计的成本，使得校准工作的进行难以被更多患者群采用。因此，这种基于脉搏波传输时间的新方法面临在不同高度时获取的脉搏波传输时间值，该方法可在不使用袖带的状态下估测个体运动前后着一个重大的挑战，即如何用一种简单而准确的方法进行校准，获取个人特征系数。

本文的目的是通过研究能引起血压或者脉搏波传输时间变化的因素（如：运动，在体表加载外部压力，引入血液静压变化）来开发一种用于无创可穿戴血压测量装置的新校准方法。

依照上述目的，我们首先进行了 2 组引起局部血压变化的实验。第一组实验引入了作用于手臂动脉的外力；第二组实验包括整个手臂抬升及测试。根据手臂抬升过程中脉搏波传输时间和手指高度之间的关系和试验结果，我们建立了一个基于生物力学的校准模型。通过抬高手臂这一简单步骤，此模型可以帮助获取个人特征系数，可用于无袖带校准。

此后我们进行了一个由 8 人参与的初步实验和一个由二十八人参与、跨时两周的试验用于测试该校准方法的正确性。两次实验均由预先静坐时的血压估测、手臂抬举的较准过程和运动后的血压估测三部分组成。测试的结果显示：1）通过使用个体的臂长和两次手指的血压变化；2）使用两组脉搏波传输时间值和一组在休息状态下的血压值，可估测个体收缩压。实验结果显示收缩压的预估误差大约是-2.8±7.7 mmHg。

该研究的结果表明使用血液静压方法在无创无袖带血压监测和校准方面具有一定的准确性，并可应用在穿戴式血压测量系统中，是一种颇具应用潜力的个人特征系数校准方法。

List of Figures

List of Tables

Table of Content

CHAPTER 1

Introduction

1.1 Current status of Blood Pressure Management

General Background

Blood pressure (BP) is the force of blood pushing against the walls of the arteries as the heart pumps out blood. The term blood pressure generally refers to arterial pressure, i.e., the pressure in the larger arteries which take blood away from the heart. Blood pressure constitutes one of the principal vital signs and is usually given in two numbers for clinical use. The systolic arterial pressure (SBP) is defined as the peak pressure in the arteries, which occurs near the beginning of the cardiac cycle; the diastolic arterial pressure (DBP) is the lowest pressure (at the resting phase of the cardiac cycle). The average pressure throughout the cardiac cycle is reported as mean arterial pressure (MBP or MAP), which can be approximated as DBP+(SBP-DBP)/3. The difference between SBP and DBP is referred as pulse pressure. Blood pressure continually changes depending on activity, posture, diet, emotional state, temperature, medication use, age and physical state, etc.

Increasing Prevalence and Low Awareness of Hypertension

Hypertension or high blood pressure, defined as of 140 mmHg or greater and/or a diastolic BP (DBP) of 90 mmHg or greater [1], is a medical condition in which the blood pressure is chronically elevated. Hypertension itself usually has no symptoms and thus people can have it for years without knowing it. However, it is a serious condition that can damage the heart, blood vessels, kidneys, eye, brain and other parts of human body, leading to coronary heart disease, heart failure, stroke, kidney failure, and other health problems. Hypertension is thus called as "silent killer".

The prevalence of hypertension is becoming a global health threatening because of the aging of population, obesity, physical inactivity and an unhealthy diet. The estimated total number of adults with hypertension in 2000 was 972 million (957–987 million), and was predicted to increase by about 60% to a total of 1·56 billion (1.54–1.58 billion) in 2025 [2]. In a statistic report update in 2006 [1], it was pointed out that in US, hypertension was listed as a primary or contributing cause of death in 2003, nearly 1 in 3 adults has high blood pressure [3], and the estimated direct and indirect cost of HBP for 2006 is $63.5 billion. In China, the prevalence of hypertension has increased by over 30% during the past decade.

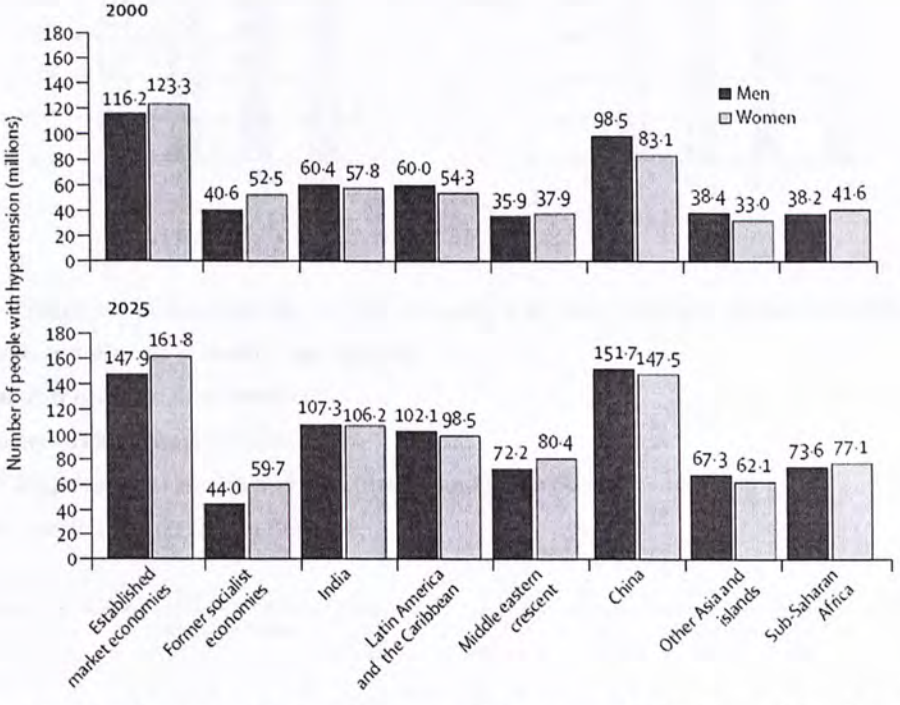

Fig. 1.1: Number of people with hypertension aged 20 years and older by world region and sex in 2000 (upper) and 2025 (lower) [2].

Despite its significance, hypertension remained mostly uncontrolled. Even in US and Canada where the control rate is higher than other countries [4], the number is still small compared with the whole prevalence (Fig. 1.2).

Moreover, it is noticed that SBP but not DBP gradually increases with age (Fig. 1.3) and the percentage of SBP hypertension is much higher than DBP hypertension (Fig.1.2), especially for adult and elderly [5, 6]. Elevated SBP imparts a predilection toward the onset of vascular events, highlighting the importance of its control.

Current philosophy ranks SBP as the most relevant component of BP for determining the risk of cardiovascular and other events in hypertensive patients, particularly those over 50 years of age. Despite its prognostic role, SBP remains more difficult to control than diastolic BP (DBP) [6].

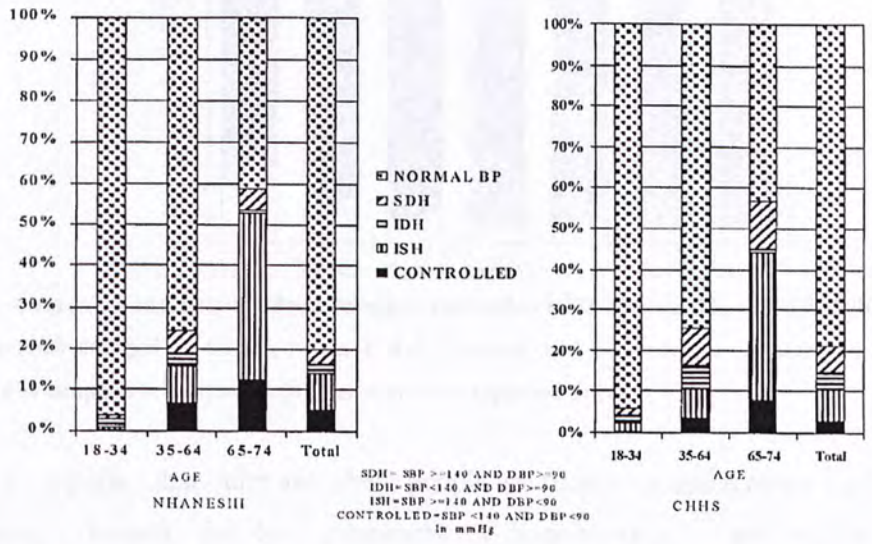

Fig. 1.2: Prevalence of elevated DBP or SBP and control by age. NHANES III and the CHHS [5].
SDH: Both systolic and diastolic hypertension;
IDH: Isolated diastolic hypertension;
ISH: Isolated systolic hypertension;
NHANES III: National Health and Nutrition Examination Survey;
CHHS: Canadian Heart Health Surveys.

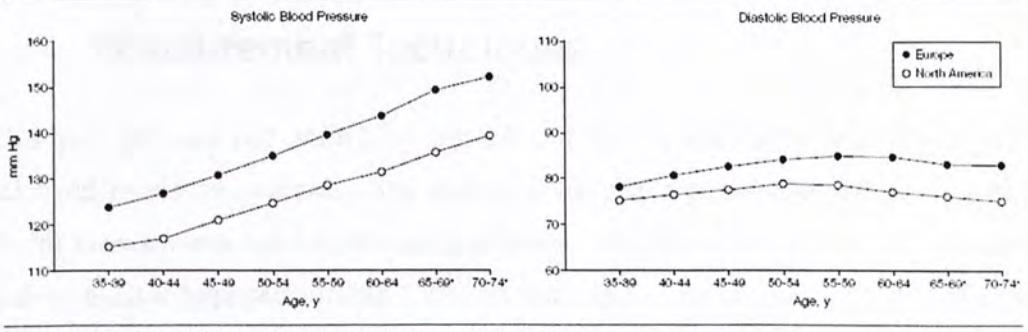

Fig. 1.3: Mean systolic and diastolic pressure in 6 European and 2 North American Countries, men and women combined by age [7].

One of the most striking features of hypertension is its low awareness. It can be noticed from Fig. 1.4 that around 30-70% of the hypertensives are unaware of their

health condition. In China this situation is serious also: around 70% of the 160 million hypertensives in China are unaware of their ailment.

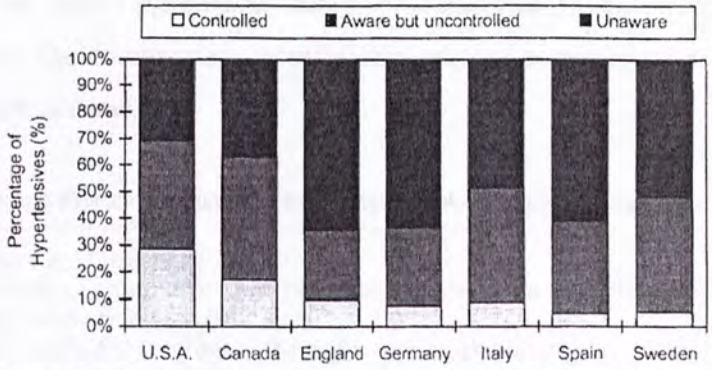

Fig. 1.4: Awareness and rate of blood pressure controlled (SBP<140mmHg and DBP<90mmHg) for hypertensives aged 35-64 yrs. in the U.S.A., Canada and 5 European countries in the past decade. The graph is re-plotted in [8] based on data reported in [4].

Ong *et al.* reported that older and obese people are more concerned about their health conditions. Indeed, the low awareness of hypertension is attributable to its asymptomatic nature. Many hypertensives, particularly young patients who do not experiencing any unusual symptoms of illness have no apparent reason to see a doctor. They may even bother to buy any BP device for home use. As a result, the detection and control of BP continues to be a worldwide public health challenge.

1.2 Current Status of Noninvasive Blood Pressure Measurement Techniques

This gap between our ability to prevent and treat hypertension and the actually achieved levels of awareness and control constitute a significant failure of public health management and health care worldwide. Bakris *et al.* pointed out five core actions against hypertension [9]. The 1st step, detect and prevent high BP (table I), indicates the serious need for a technique that is able to check BP regularly, to provide long-term monitoring, and to be adopted outside the hospital. Besides, the target group for this technique should not only include the elder who concern their health condition more consciously, but also individuals who have no apparent reason to consult a doctor and would accept portable/mobile medical devices because their normal life activities will not be interrupted.

This requirement coincides with an emerging concept termed "mobile health" (m-Health) which is an evolution from traditional desktop "telemedicine" platforms to wireless and mobile communication terminals (e.g. cellphone, PDA). To be integrated into m-Health systems, the design of medical device (BP device here) must consider factors like compactness, comfortableness and convenience as important as the measurement accuracy.

Table 1.1: Five core actions for health-care professionals (Excerpt from [9])

Detect and prevent high BP
Promote community awareness of hypertension and prevention
Measure/re-check BP
Measure BP in other settings (home, work and community)
Use accurate technique
Follow-up on elevated readings
Follow current guidelines

Cuff-based Techniques for Blood Pressure Measurement

Over past 100 years, the auscultatory method has been used as the gold standard for non-invasive BP measurement. Typically, the device for this method consists of an inflatable cuff, a mercury column and a stethoscope as shown in Fig. 1.5.

An air-filled cuff is wrapped around the patient's upper arm. Practitioner listens with a stethoscope applied over the brachial artery (distal to the cuff). The cuff is firstly inflated to a cuff pressure value over the systolic level, stopping the blood flow for a moment, and then slowly deflated. While the pressure in the cuff exceeds the SBP, the brachial artery is occluded and no sounds are heard. When the inflation pressure falls just below the systolic level, small spurts of blood escape through the cuff and slight tapping sounds (Korotkoff sounds) are heard with each heartbeat. The pressure at which the first sound is detected represents the SBP. As the cuff pressure continues to fall, more blood escapes under the cuff per beat and the sound becomes louder thus. As the inflation pressure approaches the diastolic level, the Korotkoff sounds become muffles. As they fall just below the diastolic level, the sounds disappear; this indicates the diastolic pressure [10].

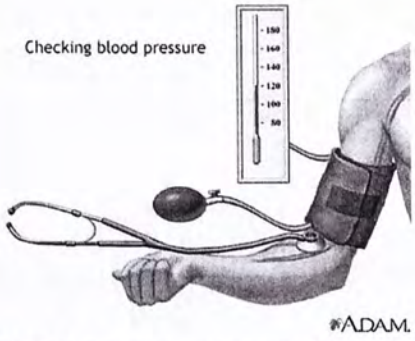

Fig. 1.5: Illustration of blood pressure measurement by auscultatory method [11].

This procedure for auscultatory method requires skill, and is difficult to automate. An alternative method, which is more easily to be used by unskilled personnel, is oscillometric method. Fig. 1.6 shows two typical oscillometric BP devices. This method is based on the principle that the oscillations of pressure pulse in the occluding cuff due to the arterial volume pulsation has the maximum amplitude when the cuff pressure is close to the mean arterial pressure (Fig. 1.7). Unlike auscultatory techniques, which measure SBP and DBP but estimate MBP, oscillometric devices measure MBP but estimate SBP and DBP. The oscillometric devices are sensitive to patient movement.

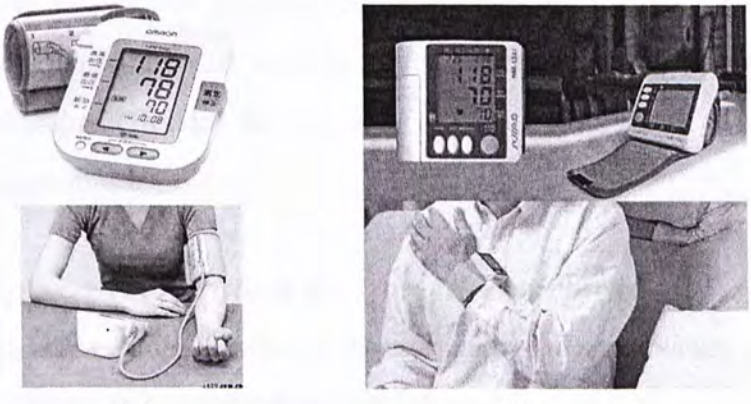

(a) **(b)**

Fig. 1.6: (a) Arm [12] and (b) wrist [13] BP monitors using oscillometric method.

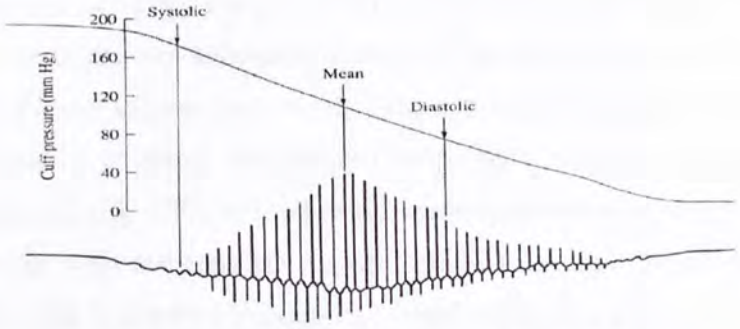

Fig. 1.7: An illustration of oscillometric method [10].

Both the ascultatory and oscillometric methods provide intermittent BP values only. Peňáz, on the other hand, proposed a continuous blood pressure measuring method (volume-clamp method) based on the principle of vascular wall unloading [14]. In this method a small inflatable cuff with photoplethysmography (PPG) sensor inside is wrapped on a finger. The cuff pressure is adjusted by a server control system according to the monitored PPG signals so that the pressure in finger cuff equals to the digital arterial pressure. This method was further developed by Wesseling [15, 16] and successfully commercialized as Fenometer®, which converts the obtained finger pressure into brachial pressure through a cuff-based calibration. Finometer is able to provide blood pressure every beat, yet its accuracy is still debatable and is under investigation. Besides, the system is too bulky and expensive to be used as home care applications.

Cuffless Techniques for Blood Pressure Measurement

The above mentioned three BP measurement techniques, i.e. ascultatory, oscillometric and volume-clamp, have a common feature that an inflatable cuff is utilized to obtain intermittent or continuous BP readings. The use of an inflatable cuff causes uncomfortable feeling and circulatory interference that might damage the arteries if frequent measurements are required. Thus other methods have been investigated in order to overcome these disadvantages. The tonometry method is one of the techniques that abandon the use of inflatable cuff. This method typically involves a transducer including an array of pressure sensors positioned over a superficial artery. Hold down force is applied to the transducer so as to flatten the wall of the underlying

artery without occluding the artery. When a pressurized vessel is partly collapsed by an external object, the circumferential tension of the arterial wall disappears and the internal and external pressures are equal. The applied pressure read from the sensor array and used to maintain the flattened shape thus indicates the arterial blood pressure reading [17]. These tonometric systems measure a reference pressure directly from the wrist and correlate this with arterial pressure using a known constant (gain). This gain is obtained through cuff-based calibration procedure and it needs recalibration if the subject moves. The accuracy of tonometric systems depends on the accurate positioning of the sensor array over the underlying artery and is decreased by wrist movements.

An alternative for cuffless and continuous blood pressure measurement is the pulse transit time (or pulse wave velocity, PWV) based method. The general principle of this method is that an increase in blood pressure will cause the stiffness of artery, and therefore increase the velocity of pressure pulse transmission through the arteries. One way to measure the pulse transit time is to place two PPG sensors along the arterial tree, proximal and distal. However, this is difficult to implement in reality because the motion artifacts and the recording force for PPG sensor on the upstream artery would affect the measured PWV [18, 19] and thus cause inaccuracy to the measurements. An alternative way is to measure the pulse transit time from the R wave of Electrocardiogram (ECG) to a feature point on the distal PPG waveform. The pulse transit time is then correlated with arterial pressure through specific models.

To summarize, within the noninvasive blood pressure measurement techniques, the ascultatory and oscillometric methods can directly obtain blood pressure values close to central arteries. A mercury column operated by trained operated physicians (ascultatory method) is regarded as the gold standard, while the oscillometric devices are more easily to be used outside the hospital. These two methods are limited for long term and continuous monitoring due to the use of an inflatable cuff and therefore other techniques have been developed to overcome this problem, e.g. volume-clamp method used by Finometer® (cuff is switched to fintertip), tonometry and pulse transit time based methods (cuffless). Yet the tonometry method which requires skillful operation for positioning the device and the volume-clamp method which costs a lot and still with inflating finger cuff, are still not suitable to be adopted for long-term monitoring. In contrast, the pulse transit time based method provides cufless and

continuous blood pressure values with compact devices, simple procedures and low power consumption. It is therefore more preferable to be further integrated into wearable blood pressure devices than any other method mentioned before.

1.3 Motivations and Objectives of This Thesis

It is noticed that the pulse transit time based method, as well as other cuffless techniques for blood pressure measurement obtain their own feature parameters from peripheral arteries instead of recording blood pressure in central/large arteries directly. Thus how to correlate these feature parameters with blood pressure becomes an essential step for blood pressure measurements based on these cuffless techniques. This step is called calibration. For the pulse transit time based technique, calibration refers to the process in which the coefficient(s) within the model for prediction is/are calculated. The calibration procedure plays a very important role in the blood pressure monitoring processes as it directly affects the prediction results and the design of blood pressure device. Therefore this study is carried out to investigate a practicable calibration method that can be further implemented for the design of PTT technique based wearable blood pressure devices.

The objectives of this study are:

1. To study the effects of factors that can induce dynamic changes in pulse transit time or blood pressure and investigate the feasible use of a factor for calibration method;
2. To develop a calibration method for BP measurements based on pulse transit time technique and to evaluate this method by compare the overall BP prediction results with reference to noninvasive gold standard.

1.4 Organization of This Thesis

This thesis has six chapters. In next chapter, some background knowledge about the arterial anatomy, the pressure related arterial elastic properties and photoplethysmography technique are given. Moreover, a review on previous calibration techniques for the pulse transit time based blood pressure measurement is presented. In chapter 3, two experiments are designed to study two factors that would possibly be utilized for novel calibration methods. In chapter 4, a bio-physical model for a hydrostatic calibration method is built up. Based on a

preliminary study of this method, a novel way of implementing this algorithm is given. In chapter 5, the hydrostatic calibration model using the modified way of implementation is investigated through an experiment in which the SBP dynamic range is enlarged by introducing exercise. Chapter 6 gives the summary of this thesis and some recommendations for future research are suggested.

CHAPTER 2

Backgrounds

2.1 Principle of the Pulse Transit Time-based Approach for BP Measurement

2.1.1 General Descriptions

When the ventricles contract and blood bursts into the aorta from the left ventricle, a pressure pulse is generated by the heart and propagates through the arterial tree with a certain speed, named pulse wave velocity (PWV). The time needed for pressure wave to transmit through a length of an artery is called pulse transit time (PTT). Fig.2.1 illustrates the pulse propagation through arteries over a certain time interval Δt. The pressure pulse wave moves with a velocity much faster than the forward movement of the blood flow itself. The average maximum velocity of blood in the aorta is 0.75m/s and 0.25m/s in the carotid artery [20] and slows down to several mm/s in the peripheral arterioles. PWV is relatively low for young subjects whose arteries are more distensible [21, 22] and gradually increases when the pulse moves from the aorta to the periphery for each individual [23]. For the aorta of young healthy subjects the PWV is of the order of 5 m/s and for elderly people, it can reach 15 m/s in the periphery [23, 24].

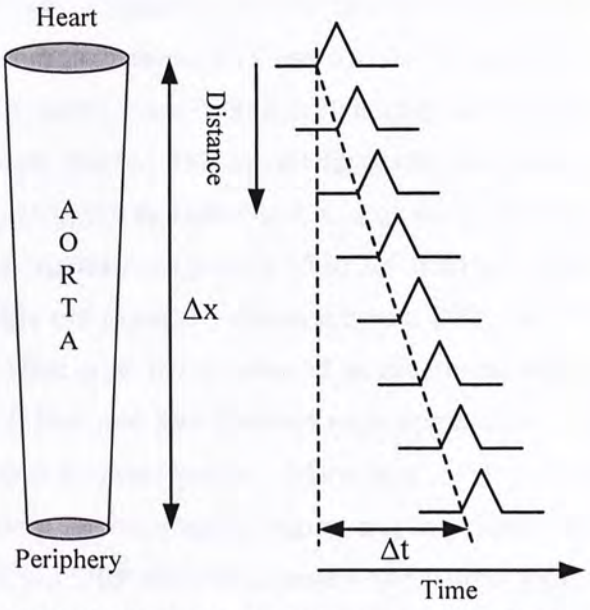

Fig. 2.1: Schematically illustration of pulse wave velocity and pulse transit time.

PWV is related to the physical properties of arterial vessel. It carries the information of arterial stiffness and has been proclaimed as an important parameter in the analysis of the behavior of arterial tree, since various diseases are known to change the stiffness (or elasticity) of the arteries [25-27]. For example, atherosclerosis causes the arterial wall to become thicker and harder, and narrows the arterial lumen [28]. Many investigations have been conducted based on the studies of PWV, which relate the effects of aging and vascular diseases to vessel pathology and distensibility [29-33].

Interestingly, the physical properties of arterial wall that relate to PWV (or its inverse, PTT) are pressure-dependent. Arterial blood pressure reflects not only the above mentioned vascular diseases, but also important pathological information of acute and chronic cardiac diseases. The novel technique for arterial blood pressure measurement based on PTT has been proposed and has drawn much attention because it provides cuffless and continuous BP while only requires easy measuring procedure and simple devices. This technique is based on the fact that an increase in arterial blood pressure (BP) tends to stiffen the arterial wall and thus results in the increasing of PTT.

Research studies have been done to investigate the relationship between PTT and BP. Steptoe [34] showed that PTT and mean blood pressure has a highly negative and reliable relationship under the effects of vasodilator drug and a series of mental and

static physical activities. Obrist *et al.* [35] induced cold and metal stimulations to examine the relationships between PTT and SBP/DBP separately. They found that SBP showed large dynamic range from 8 to 20 mmHg and was highly correlated with PTT, while DBP only showed limited variations and was less correlated with PTT. Geddes *et al.* [36] conducted an experiment on dogs using nerve stimulus and drugs to induce a large DBP dynamic range from 15 to 200 mmHg. In this study PWV was found to have a high and negative relationship with DBP, and PTT was nonlinearly related to DBP. Allen *et al.* [37] conducted an experiment on hypertensive patients and pointed out that PTT and SBP covaried more appreciably in these hypertensives than in normotensives reported before. Marie et al. [38] carried out an experiment including mixed dynamic and static exercises, and they found that during the mixed exercise, both SBP and DBP showed increased correlations with PTT compared with those measured at rest. Payne [39] showed that PTT is highly related to SBP under the effects of vasodilating and vasoconstricting drugs' effects, while PTT' which is the vaso-component of PTT showed better relationship with MBP and DBP.

In general, this novel technique will be completely non-invasive and cuffless. It can provide continuous and long-term measurement for intermittent or beat(s)-to-beat(s) BP and BP variations. It is also able to be integrated into wearable healthcare systems which can be used in telemedicine and preventing strategy for healthy people. These advantages fill in the gap left by traditional BP monitoring devices, lighting up new directions on clinical diagnosis and treatment.

2.1.2 Pressure Wave Propagation in Cylindrical Arteries

The fundamental concept of relating BP with PTT rises from the basic models of pressure wave propagation in arteries, named M-K equation and Bramwell-Hill equation.

Moens and Korteweg expressed PWV as a function of the elastic modulus of the artery wall (E), the thickness of the arterial wall (h), the inner radius of the artery (r) and blood density (ρ) for a thin-wall elastic tube containing incompressible non-viscous fluid (known as M-K equation) a:

$$PWV = \sqrt{\frac{Eh}{2\rho r}} \tag{2.1}$$

Hughes *et al.* [40] showed that the elastic modulus E increases exponentially with the

increasing mean blood pressure P,

$$E = E_0 e^{\alpha p} \tag{2.2}$$

where E_0 is the zero-pressure modulus and α is a constant that depends on the particular vessels (typically $0.016<\alpha<0.018$). By substituting equation (2.2) into (2.1) it relates the PWV with BP. However, most of the variables in these two equation are very difficult to be measured. Bramwell and Hill [20, 21] adapted the M-K equation to another expression that relates PWV with the compressibility of blood that flows in arteries,

$$PWV = \sqrt{\frac{V}{\rho}\frac{dP}{dV}} \tag{2.3}$$

where V denotes the blood volume.

Compressibility is a measure of the relative volume change of a fluid (i.e. blood) as a response to a pressure (i.e. MBP) change. It is given by the inverse of the bulk modulus (K) of a substance (i.e. blood):

$$K = -V\frac{dP}{dV} \tag{2.4}$$

From the definition it is noticed that the bulk modulus of blood describes the volume-pressure (V-P) relationship of blood.

Though M-K equation is based on elastic modulus of artery wall (E) while Bramwell-Hill equation is based on bulk modulus of blood (K), the two can be converted with the relationship between E and K presented by Posey and Geddes [41]. Since the blood V-P relationship that can be mathematically modeled is much easy to obtain, the Bramwell-Hill equation is selected in my study to relate PTT with blood pressure by further substitute

$$PTT = \frac{L}{PWV} \tag{2.5}$$

into (2.3), where L is the vessel length it takes a pressure pulse to travel with certain PWV.

2.1.3 Determining the PTT for BP Measurement

As presented in equation (2.5), PWV can be theoretically calculated by measuring the length of a certain distance L along the artery and the tracking the time delay for a

pressure pulse to travel through this distance. PWV can be measured invasively by inducing two pressure transducers at the two site of an artery [42, 43] or non-invasively by other techniques, e.g. external pressure transducers [44], Doppler ultrasound [30, 33, 45] and photoplethysmography [46, 47]. Noticing that the L is difficult to measure, a common way is to measure the PTT and calibrate the other constant parameters that appear in the PTT-BP model. Recently the photoplethysmography (PPG) technique has been widely developed and used for PTT measurement.

Photoplethysmography

Photoplethysmography is an optical means for recording the volumetric change of blood within the arteries of skin [48]. This method was later validated for estimating both skin blood flow and blood volume changes [49].

The main recorded event of PPG is the blood volume pulse, i.e. the expansion of vessel produced by the arrival of pressure pulse. As the pressure wave front travels down the arterial system, the transient increased pressure at the wave front causes the elastic arterial walls to expand, thereby accommodating an increased blood volume over quiescent. Typically, vessel wall expansion and shrinkage results in blood volume change, which can reveal the pulsatile propagation of pulse waves along the vasculature. The hemodynamic properties of the vasculature, such as arterial elasticity, resistance and leakage, together with the inertia of the blood itself, will affect the shape of the detected PPG waveform.

After its development, PPG has been widely utilized in the study of the peripheral pulse wave characteristics [50], monitoring of the peripheral circulation [51], heart rate and respiratory rate [52, 53]. Besides these applications, the clinically widely used pulse oximetry devices (SpO_2) utilize two different wavelengths of PPG signals to calculate the oxygen saturation rate of blood hemoglobin.

PTT Recorded for BP Measurement

According to its definition, PTT should be calculated as the time difference between the occurrences of the same pulse arriving at two sites along the same artery [54]. However as pointed out in [34], this measurement approach has two disadvantages: firstly, it is difficult to monitor the trains of artefact-free pulses from two sites continuously, and secondly the time interval between them is very short and therefore,

this measurement is susceptible to errors. To overcome these mentioned problems, the characteristic points like the Q wave and R wave of electrocardiogram (ECG) have been investigated to use as the trigger and the pulse transit time was measured from the trigger to to the arrival of the pulse at a peripheral site [34, 35]. The pulse transit time initiated by the R wave of ECG is named as PTT in this dissertation.

It should be noticed that PTT measured from R wave of ECG includes a time interval called pre-ejection period (PEP). PEP starts from the electrical depolarization of the heart and ends with the opening of the semilunar valve when blood is ejected into the aorta. Thus PEP includes both the electro-mechanical delay and period of isovolumetric contraction of cardiac muscles [34, 35, 54]. It ranges from around 12% to 35% of PTT [39] and is traditionally measured invasively by catheters or calculated non-invasively by using impedance cardiography technique. In order to differentiate the two time delays, the pulse transit time calculated from aorta to the periphery is named as PTT' in this thesis. Fig. 2.2 illustrates the difference between the two time intervals.

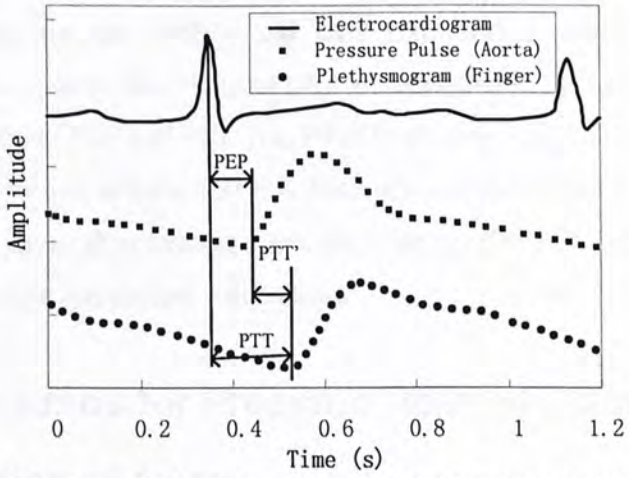

Fig. 2.2: Definition of the pre-ejection period (PEP), pulse transit time (PTT') and pulse transit time measuring from the peak of ECG R-wave (PTT).

As shown in Fig. 2.2, PTT is the sum of PEP and PTT'. Although both the M-K and B-H models are developed based on PTT', many investigations are in support of using PTT instead of PTT' for BP estimation due to a higher correlation found between PTT and BP [38, 55]. There is no definite conclusion on which time interval should be used for the estimation of BP. A study for the correlations between mean blood pressure (MBP), systolic blood pressure (SBP), diastolic blood pressure (DBP), PTT'

and PTT was conducted under the effects of various vasoactive drugs [39]. It is addressed in [38, 39] that PTT' is more correlated to MBP and DBP, while PTT initialed from ECG is highly correlated with SBP. This is possibly because the two components of PTT, PEP and the time it takes the pressure pulse travel from aorta to periphery (PTT'), are both inversely related to SBP. Under the situation, e.g. exercise, when SBP is greatly increased, there often induces a significantly increase in pulse wave velocity within arteries since the arterial wall becomes rigid and thus a decrease in PTT'; on the other hand, exercise induces a significant increase in heart rate due to the regulation of central nerve system, and the acceleration of heart rate is accompanied by the reduction of PEP. That is, the two components of PTT (i.e. PEP and PTT') are both inversely related to SBP and thus SBP is better represented by PTT.

On the other hand, the case for PEP and DBP is a little different. As mentioned above, PEP includes the time for isovolumetric contraction of cardiac muscles against the pressure in the aorta before the aortic wave opens. This pressure is called afterload, i.e. the pressure in the aorta at the end of diastole, which is closely related to the system arterial pressure (MBP) and DBP (the lowest pressure at diastole). Therefore there are chances that PEP and DBP are changing in the same direction and thus the combination of PEP and PTT' (i.e. PTT) bears lower correlation with DBP.

Considering these factors and the fact that DBP often demonstrates a small dynamic range during our physical activities, I am focusing on the ECG initiated PTT for systolic blood pressure estimation in this thesis.

2.2 Backgrounds for Pressure Related Elastic Properties of Artery

2.2.1 Transmural Pressure and Its Components

Transmural pressure (P_{Tr}) is defined as the difference between the intra-arterial mean pressure and the external pressure. P_{Tr} is a major factor affecting the arterial wall property:

$$P_{Tr} = P_I - P_H - P_E \qquad (2.6)$$

where P_I is the pressure inside the artery (i.e. arterial blood pressure) and P_H is a

hydrostatic component of arterial pressure produced by the vertical change of height calculated from measuring site (e.g. peripheral arteriole) to reference site (e.g. brachial artery). P_H can be approximated as $P_H=\rho gH$, where ρ is the blood density, g is the acceleration due to gravity and H is the vertical height between measuring and reference site. P_E is the pressure that is externally applied onto artery (e.g. atmosphere pressure, cuff pressure during inflation and deflation for traditional BP device or the contact pressure between digital artery and sensors).

The realistic meaning of equation (2.6) is that P_I can be obtained through this equation when other pressure components are measurable and $P_{Tr}=0$ according to the volume-pressure relationship (V-P) of blood vessel. As shown in Fig. 2.3 [56, 57], the change of volume varies across different operating point of P_{Tr}. The maximum arterial pulsation occurs approximately when the P_{Tr} is zero (unloaded status). Away from this point, the arterial pulsation begins to diminish because the artery wall is occluded or distend by excessive external or internal pressure. This is a well-known principle used in the oscillometric BP measurement devices.

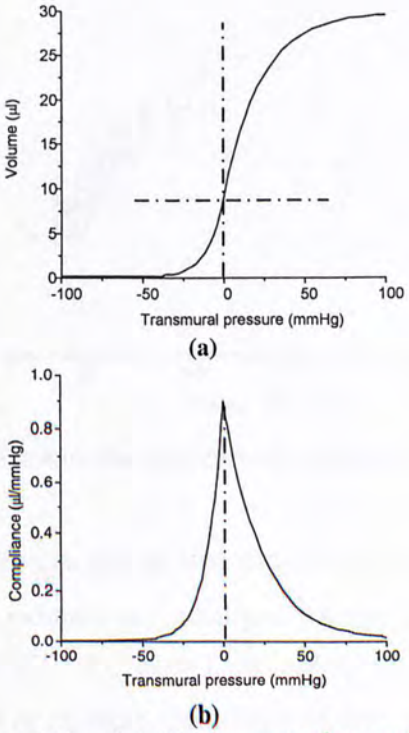

Fig. 2.3: Exponential model of (a) transmural pressure versus volume relationship and (b) corresponding compliance curve [56, 57].

2.2.2 Volume-pressure Models

The elastic parameters in discussions, such as compliance, elastic modulus or distensibility of the vessels, depend strongly on the volume change in terms of the P_{Tr}. A typical pressure-diameter relationship is presented in Fig. 2.4. The diameter data were obtained by the ultrasound transducer while the pressure values are from the FINAPRES® cuff placed on adjacent fingers. The vertical and horizontal bars are corresponding measurement errors associated with each data point. It could be observed clearly that the arterial diameter and pressure are nonlinearly related in a sigmoid shape.

Many models had been reported to describe the relationship between the diameter (or cross-section area or blood volume) of arteries and P_{Tr} [56],[58-69].

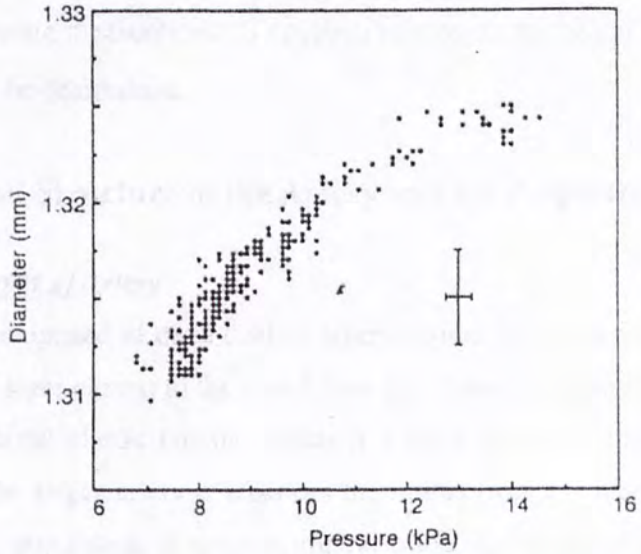

Fig. 2.4. Pressure-diameter curve of a digital artery [58].

The fitted models from in vitro and in vivo experiments have demonstrated that the V-P relationship mainly exhibits an arctangent characteristic [58, 61, 65] or an exponential characteristic [59, 60, 62-64], depending on the arterial segment and pressure range studied. For example, the arctangent model was fitted originally from the data of human thoracic and abdominal aortas [61].

$$S = A_m[\frac{1}{2} + \frac{1}{\pi}\tan^{-1}(\frac{P - P_0}{P_1})] \qquad (2.7)$$

where A_m, P_0 and P_I are three independent parameters to be estimated for each arterial segment. A_m is the maximum cross-section area of the aorta at high pressure, P_0 is the P_{Tr} at which the compliance curve reaches its maximum and P_I represents the steepness of rise of the curve and therefore compliance. At pressure level $P_0 \pm P_I$, the compliance of the vessel is reduced to one-half of its maximum value.

Shaltis *et al.* [70] charactierized this nonlinear relationship using the sigmoid curve:

$$V = \frac{b_1}{1+\exp[-b_2(P_{Tr})]} \tag{2.8}$$

where b_1 and b_2 are parameters with units of volume and inverse pressure, respectively. They explored the limitation when $P_{Tr} << 0$, when b_1 can be calculated with the volume recorded from PPG signals. By superimposing a known hydrostatic perturbation input onto a slowly varying hydrostatic pressure, defined to be the height at which the pressure measurement is acquired relative to the height of the heart, the parameter b_2 can be determined.

2.2.3 Types and Structure of the Artery and Its Properties

Structure and Types of Artery

Arterial wall is comprised of three distinct layers: intima, media and adventitia. The intima forms the layer closest to the blood flow and consists of a lining of endothelial cells. The internal elastic lamina, which is a band of elastic tissue, found most prominently in the larger arteries, separates the intima from the media. The media contains a dense population of smooth muscle cells, organized concentrically, with bands or fibers of elastic tissue. The Adventitia contains collagen and functions to add rigidity and form to the blood vessel.

Systemic arteries can be subdivided into two types; muscular and elastic; according to the relative compositions of elastic and muscle tissue in their tunica media as well as their size and the makeup of the internal and external elastic lamina. The larger arteries (diameter >1cm) are generally elastic and the smaller ones (0.1-10mm) tend to be muscular. Systemic arteries deliver blood to the arterioles, and then to the capillaries, where nutrients and gasses are exchanged.

In general, the overall mechanical properties of the arterial wall are determined by

how different compositions of collagen, elastin and protein are linked. The general rule is that when the elastin ratio is higher than the collagen ratio, the elastic modulus decreases and distensibility increases and vice versa [71]. The structures of arteries from central to peripheral are shown in Fig. 2.5.

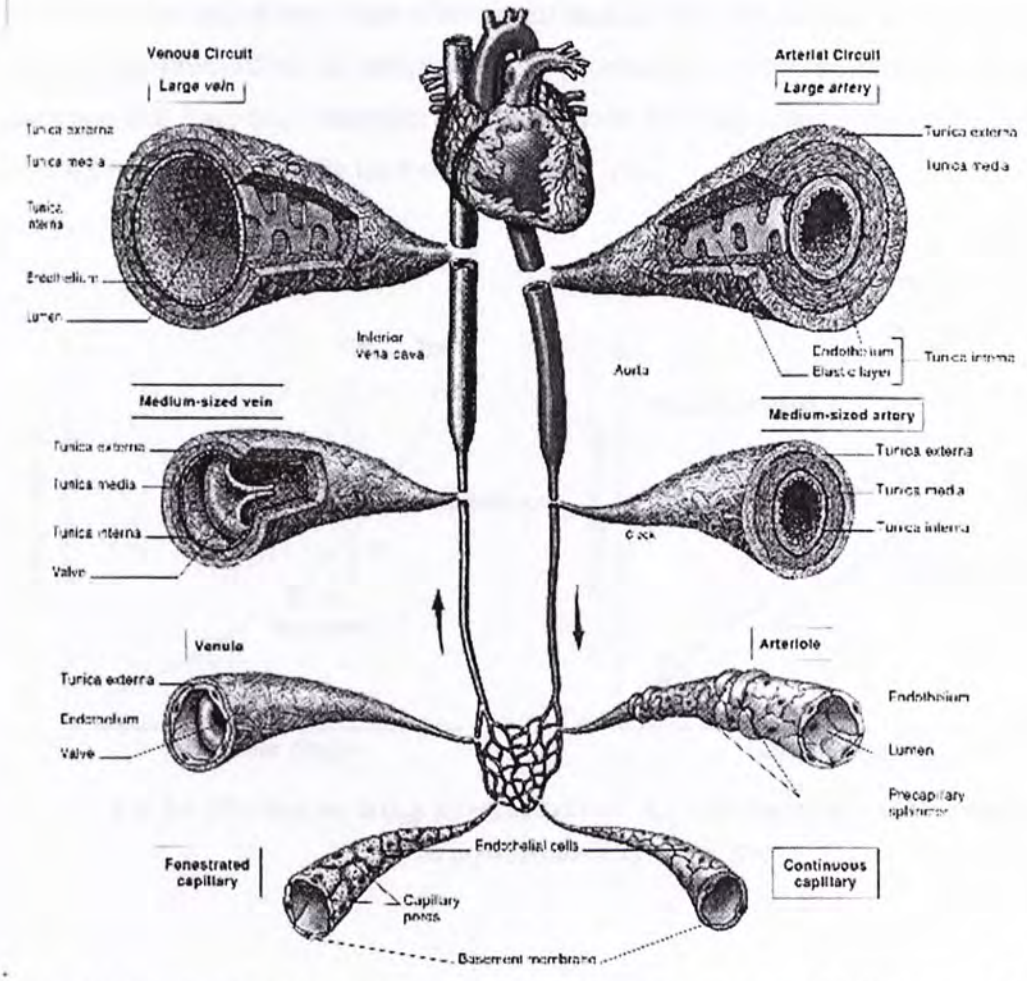

Fig. 2.5: Human circulatory system, showing some of blood vessels and their structures [72].

The properties of arterial wall are affected by different reasons, e.g. acute or chronic factors. An increase in stiffness (or elastance) related to arterial wall composition occurs over a long period of time, e.g. with advance age, hypertension and arteriosclerosis, and shifts the pressure-diameter curve to the left increasing its slope (Fig. 2.6 left). Acute changes can, however, occur in elastic arteries with changes in distending pressure but these changes are passive and the movement is along the same pressure-diameter curve. For example, during vasodilation both pressure and diameter decrease in elastic arteries causing a passive decrease in wall stiffness and

the slope of the pressure-diameter curve. A change in stiffness of muscular arteries is primarily due to acute changes in smooth muscle tone and causes shifts of the pressure-diameter curve (Fig. 2.6 right). During vasodilation diameter increases while pressure decreases causing a decrease in stiffness and a shift of the curve to the right; vasoconstriction increases stiffness and has the opposite effect. Advancing age and hypertension have little effect on stiffness of muscular arteries in humans and drugs have little effect on stiffness of elastic arteries. However, recent evidence indicates that long-term treatment with cholesterol-lowering drugs may reduce large elastic artery stiffness while increasing diameter [73].

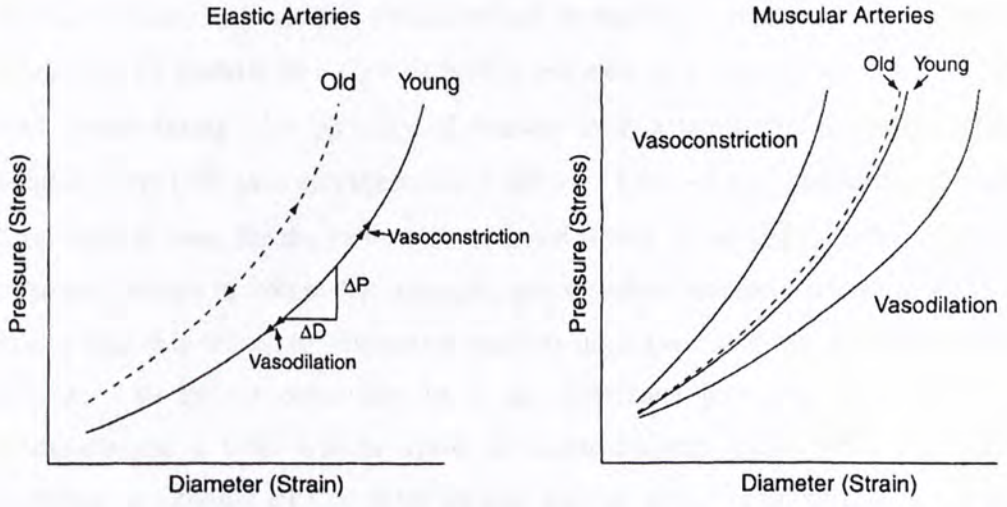

Fig. 2.6: Effects of acute (e.g. aging) and chronic (e.g. vasoconstriction and vasodilation) factors on pressure-diameter vurves [74].

2.3 Literature Review on the Calibration Methods for Cuffless Blood Pressure Measurements

As discussed in [37, 38], the regression slopes for BP and PTT vary across subjects. Previously researchers have developed different models which could describe the observed relationship between BP and PTT and could be further used for estimating BP. Most of these models contain subject-dependent parameters and therefore a challenge of the PTT-based BP measurement techniques is how to calibrate it individually.

To calculate these model parameters, traditional methods then take use of one or more known PTT and BP sets, where BP is obtained by the conventional cuff-based devices. There have been some papers and hundreds of patents discussing the topic about calibration techniques. According to the number of BP and PTT pairs used, these approaches are defined as multipoint, one point and cuffless (i.e. no reference BP is needed) calibration in this thesis. For one point calibration method different models and methods are used so that only one pair of $\{PTT_0, BP_0\}$ can solve all parameters in the model [75-77]. Chen [77, 78] proposed an expression that $BP=a+b \cdot \ln(T)$ and they further found two methods to calculate a and b given one pair of $\{PTT_0, BP_0\}$: (1) a and b are highly correlated linearly so that a can be expressed by b and two predetermined constants; (2) parameter b is moderately related to PTT linearly ($b = C_3 \cdot PTT_0+C_4$) and then the C_3 and C_4 are obtained from least square fitting of a plurality of datasets from a number of subjects. Nihon Kohden Corp. [75] gave an expression of $BP = \alpha \cdot PTT + \beta$ and they further provided three embodiments for the calibration of α and β with given $\{PTT_0, BP_0\}$: (1) α is a parameter relates to volumetric elasticity and therefore inversely relates to PTT; (2) pulse pressure is related to volumetric elasticity during rest so that α is related to pulse pressure. To further determine the α, an experiment including 46 subjects was conducted and a table was provided in which different values of α were given according to different PTT or pulse pressure ranges. The 3rd embodiment is that they assumed that α equals to the ratio of hydrostatic pressure change induced by postural change and the corresponding PTT change. Other one point calibration methods include using a pair of $\{PTT_0, BP_0\}$ and a fixed slope/constant to calculate the constant/slope given the linear BP-PTT expression. These kinds of calibration methods often involves a series of coefficients predetermined empirically or by preliminary experiments, or assumed conditions that were observed from preliminary experiment only. However this is questioned by researchers since there still has no definite confirmation on whether these empirical coefficients/assumptions are still valid in different subject pools.

On the other hand, the multipoint calibration process usually involves some procedures during which the PTT and BP are recorded and later submitted into the proposed models to calibrate the coefficients for each individual. Comparing with one point calibration, this kind of calibration method usually involves less

predetermined constants but utilizing prior {PTT, BP} values during some activities that could introduce large BP range. These procedures may include a long time monitoring of BP and PTT during resting condition [79], an exercise session [80], hydrostatic pressure changes [81-83] and a stress test [84], etc. Besides, in some studies that presenting linear models of PTT and BP relationship, the slope [85, 86] or the intercept [87] is fixed while the other one is calibrated using measured {BP, PTT} values. An obvious disadvantage for multipoint calibration methods is that they often rely on procedures which are not easy to be performed (e.g. running, tilting) or involve extra bulky equipment (e.g. treadmill, expiration machine), thus their use are most limited to research purpose only.

In an attempt to overcome this shortcoming, recent research focuses have been on the direction towards calibration approaches that eliminate the use of cuff-based BP device, or explore more information about the BP-PTT relationship during one measurement using a cuff-based BP device. These two directions could be briefly explained through understanding the concept of transmural pressure (P_{Tr}) and its components discussed in 2.2.1.

The zero P_{Tr} is corresponding to the maximum arterial compliance (C, and C=dV/dP) where the maximum arterial pulsation could be observed. To trace this specific instance, the study in [70] used this phenomenon and recorded the PPG on the finger of the subject while he/she was asked to move his/her hand vertically above and below heart level.

The results of these studies thus indicate that changing the internal hydrostatic BP (P_H) or externally applied pressure (P_E) can induce changes in PTT and that the relationship between PTT and P_E or P_H can be used in calibration or estimation. The drawback of method about changing P_E proposed in [88, 89] is that a cuff-based measurement of BP is essential and therefore not suitable if a cuffless calibration process is expected.

Up to the present only limited work has been done towards the cuffless calibration approach. In [81] changes in hydrostatic pressure induced by different hand postures were used for the estimation of BP. They proposed that changes in PTT was corresponding to $\frac{1}{2}\rho gh$ pressure variation due to arm posture changes. Still, their approach in [81] requires an initial BP reading from the conventional cuff-based devices. Another group [90] made use of changes in hydrostatic pressure induced by different postures (supine, sitting or standing) to estimate BP. In their work the

near-linear relationship between changes in hydrostatic pressure and corresponding changes in PTT was obtained through posture changing procedures. The slope of this relationship was then used as the slope in the linear equation describing arterial BP and PTT, while other parameters were calculated by an initial use of cuff-based BP measurement. Our research group further proposed a cuffless method for mean blood pressure (MBP) estimation [91]. In this work a mapping algorithm was developed based on theoretical simulation results of the hydrostatic calibration model in [92] to transfer the ratio of PTT changes and arm length to mean arterial pressure.

2.4 Section Summary

In this chapter the principle of PTT based technique for BP measurement is introduced and a brief review on previous studies on PTT-BP relationship is provided. Moreover, the structure and related properties of arterial wall as well as how does the elastic properties of vessel wall relate to BP are given to provide the background for this PTT related method. After presenting the basic background physiological and physical knowledge, I further raise the challenge of the PTT-based technique for BP measurement, i.e., the calibration procedure. A review on previous calibration methods documented in paper and patent for PTT/PWV related approaches for BP monitoring is given in this chapter.

CHAPTER 3

Investigations on Factors Affecting PTT or BP

As presented in chapter 2, many previous calibration methods make use of the relationship between PTT (or BP) and those parameters which need to be calibrated by observed during resting status or physical activities. Noticing that those would introduce extra devices or excessive BP measurements to the calibration procedure, I chose to study factors which are related to transmural pressure (P_{Tr}) since the elastic property and one of its representations (i.e. PTT) are P_{Tr} dependent. The two selected factors are external pressure (P_E) and hydrostatic pressure (P_H). The effects of these factors on PTT or BP will be presented and the possibilities of utilizing these factors for calibration procedure will be discussed as well.

3.1 The Effects of External Pressure

3.1.1 Background

In 1886, Riva-Rocci introduced the pressure cuff for the measurement of SBP and DBP by the detection through palpation of the pressure pulse distal to the cuff. The sounds, which originate from the blood flow under the cuff when the cuff pressure is between SBP and DBP (Korotkoff Sounds), and the oscillations of pressure pulses under a pressure cuff founded the basis for auscultatory sphygmomanometry and oscillometric BP device. For cuff pressure between DBP and SBP, the artery under the cuff is occluded when arterial blood pressure is below the cuff pressure and open when arterial blood pressure is greater than the cuff pressure.

The external pressure from a Riva-Rocci cuff is only one format of the P_E. P_E can be

applied to different site along the arteries and its effects on local or downstream flow and pressure pulse transmissions have been examined in limited studies. Driscoll *et al.* [18, 19], with their purpose on determining an appropriate recording force for the non-invasive pressure pulse recording techniques, fixed the force applied to radial artery and varied the force applied to brachial arteries discretely over a certain ranges according to the pre-measured pressure for each subject. Meanwhile, they measured pulse amplitude, contour, relative transmission ratio and pulse wave velocity (PWV) over the different applying force. In their study the various recording force was provided by a pressure sleeve and the pressure pulse related signals were monitored by pulse Doppler ultrasound technique and piezoelectric pulse transducers. It was found that PWV decreased significantly ($p<0.021$) with applied force on brachial artery higher than around 60% of the largest recording force, which is the force measured when the finger pressure pulse is about to disappear. Nitzan *et al.* [93] investigated the effects of external pressure applied by upper arm sphygmomanometer cuff on downstream distal arteries during the slow decrease of cuff air pressure. They recorded PPG signals from index fingertips of both hands. The ratio of these two PPG amplitudes and the time delay between these two PPG signals were monitored in order to interpret the changes in the compliance of conduit arteries and small arteries with cuff deflation. Teng *et al.*[94] reported significant changes in PTT measured from ECG R wave to fingertip PPG when different degrees of the contact force were applied to the transducer using a contact-type PPG acquisition device.

As introduced in chapter 2, the pressure applied externally onto the arteries (i.e. P_E) could change the transmural pressure and thus the pressure-dependent elastic properties of arterial wall characterized by PTT, providing extra information of the PTT-P_E relationship over a large pressure range (from zero to over SBP). Noticed that all of current calibration methods demand the initial use of one or multiple blood pressure values from the traditional cuff-based BP device, it is valuable to investigate this process and the PTT-P_E relationship. Up to the recent, there has no investigation on the pressure recorded in the Riva-Rocci cuff and the PTT measured from ECG and finger PPG from the same hand. Therefore, I conducted an experiment to study the effects of external cuff pressure on PTT during both the inflation and deflation processes.

3.1.2 Experimental protocol

Sixteen healthy subjects, aged 18-32 years including 10 males, participated in this study. Subjects were asked to refrain from coffee and alcohol 2 hours before the experiment.

ECG and PPG signals were obtained from subjects' fingertips by stainless steel electrodes and a pair of light emitting diode and photodetector (IR91-21C. and IR91-21B, Everlight, Taiwan), respectively. A mercury sphygmomanometer was connected to the automatic blood pressure (BP) meter (Omron HEM-907) via a Y-tube and the cuff was wrapped around the ipsilateral upper arm of the subject. BP was measured by the automatic BP meter and simultaneously by an experienced nurse using the mercury sphygmomanometer at the beginning and the end of the experiment. All measurements were obtained with a sitting posture. The experimental setup is shown in Fig. 3.1.

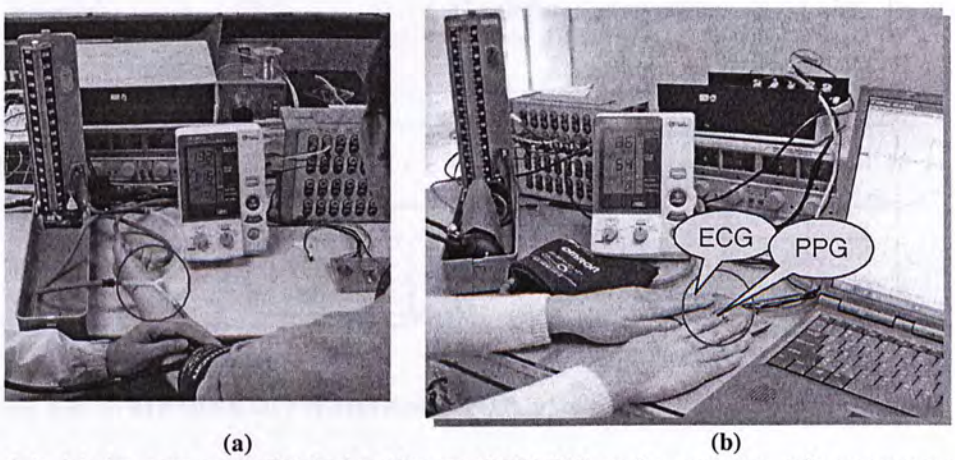

(a) (b)

Fig. 3.1: (a) An automatic BP device (Omron HEM-907) and a mercury sphygmomanometer connected by a Y-shape tube (in red circle), and (b) Circuits for obtaining ECG and PPG from the fingertips of a subject.

For each subject, the averaged BP values taken at the beginning of the study were used as the reference and eight levels of cuff pressure (P_{cuff}) were predetermined, i.e. 0mmHg, 40mmHg, 80% of diastolic BP (DBP), DBP, and 25%, 50%, 75% and 100% of pulse pressure (PP, the difference of systolic and diastolic BP) above the DBP. Note that the last level, 100% of PP above DBP, is equivalent to the reference systolic BP (SBP) obtained at the beginning of the study.

ECG and PPG signals were recorded for 20s when P_{cuff} was directly raised to each

pressure level (i.e. during the inflation process). The cuff was completely deflated and the subjects were allowed for a 1 min. rest in between recordings. Another 7 datasets were recorded at each P_{cuff} (except for P_{cuff}=SBP) when P_{cuff} was first raised above SBP and deflates to the desired level (i.e. during the deflation process). The experimental protocol was shown in Fig. 3.2.

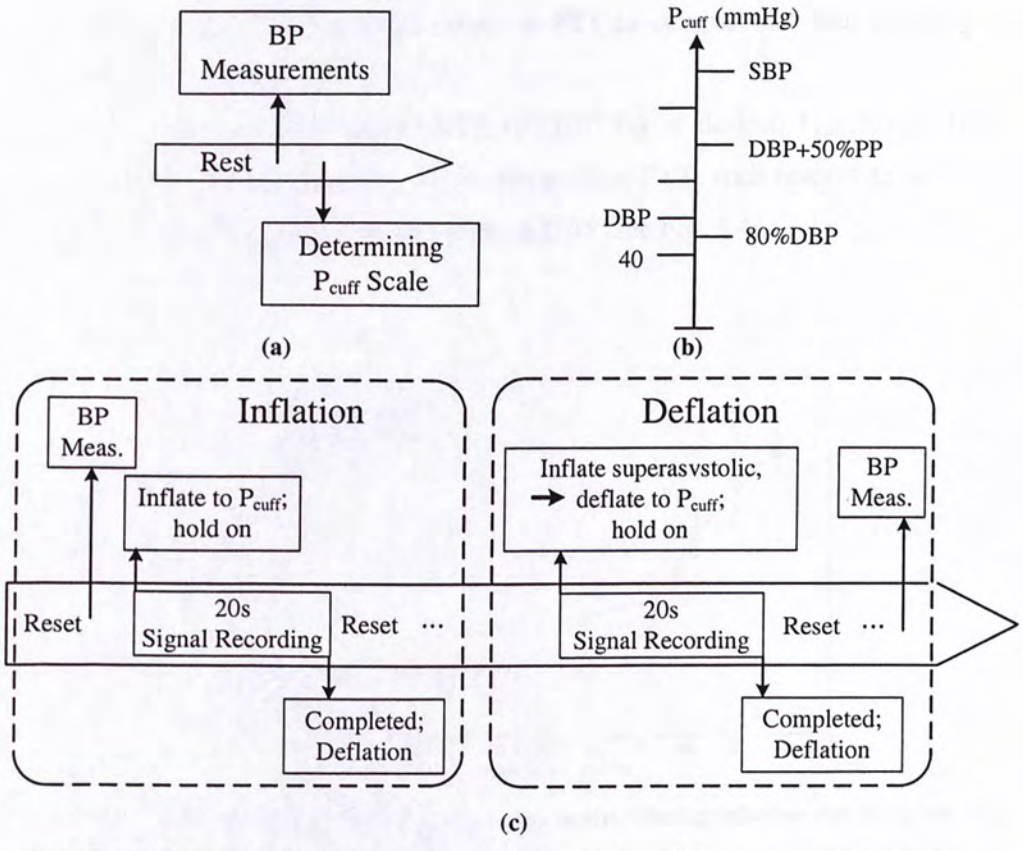

Fig. 3.2: (a) Procedure for Pre-experiment, (b) P_{cuff} scale, and (c) experimental procedure.

In this study, PTT was measured as the time interval between the peak of R wave of ECG and the upstroke of the PPG pulse in the same cardiac cycle. Results were presented as mean±standard deviation. The paired Student's t-Test was used to compare the difference between two variables, and $p<0.05$ was considered statistically significant. For each subject, the mean PTT obtained at all P_{cuff} during inflation were compared with those obtained during deflation. Overall, the averaged normalized PTTs of all subjects obtained during inflation and deflation were also compared.

3.1.3 Analysis for the Effects of External Pressure on PTT

As shown in Fig. 3.3, PTT maintained at a relatively stable level over a certain range of P_{cuff}, but significantly increased with larger cuff pressures. When P_{cuff} was maintained at a level around the SBP, the pulse was hardly noticeable on all subjects and PTT could only be obtained from 10 subjects. For P_{cuff} equals to DBP+75%PP, an increase of 75.3±19.8 ms was found in PTT as compared to that obtained when P_{cuff} equals 0 mmHg (PTT_0).

Fig. 3.4 showed the normalized PTT (PTT/PTT_0) at desired P_{cuff} levels from all subjects. Significant differences in the normalized PTT, with respect to unity, could only be observed after P_{cuff} reached 80% of DBP (see Fig. 3.4).

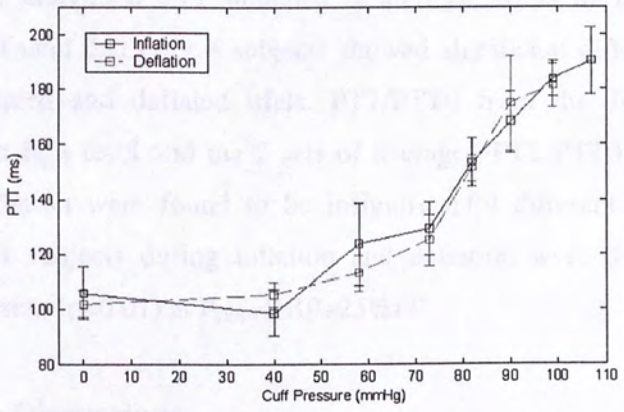

Fig. 3.3: PTT values at different P_{cuff} from one subject during inflation and deflation [95].

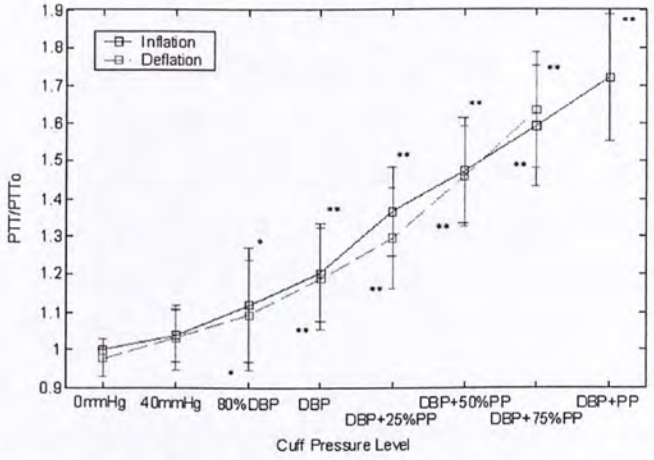

Fig. 3.4: Mean of normalized PTT at predetermined P_{cuff} levels during inflation and deflation from 16 subjects. (Trials with * implies the mean PTT was significantly different ($p<0.05$) from PTT0. Trials with ** denotes $p<0.0001$) [95].

When comparing individual PTT obtained at all P_{cuff} levels during inflation and deflation, it was found that only 4 subjects showed significant differences ($p<0.05$) between the inflated and deflated trials. PTT/PTT0 from the 16 subjects were averaged for each P_{cuff} level and the 2 sets of averaged PTT/PTT0 obtained during inflation and deflation were found to be insignificantly different ($p= 0.9$). PTT obtained from all subjects during inflation and deflation were only found to be significantly different ($p=0.01$) at P_{cuff}=DBP+25%PP.

3.1.4 Section Discussions

Regardless of the differences in the study protocol, the trend of PTT changes observed in this study as a result of applied cuff pressure was consistent with that previously reported in [19, 93]. The monotonically increase of PTT with cuff pressure applied over brachial artery could be an indication of changes in artery properties, e.g. the arterial distensibility (the ratio between arterial compliance and the arterial blood volume). As PTT in a conduit artery is related to arterial distensibility according to Bramwell-Hill's equation [96], the applied cuff pressure will ultimately result in an alteration of PTT. Yan *et al.* [97] newly described PTT as a function of cuff pressure during the process of upper cuff deflation.

Moreover, different from all the previous studies, this study also compared PTT

obtained when P_{cuff} was directly increased to a predetermined value with those obtained when P_{cuff} was first raised above the SBP and then deflated to the predetermined value. In general, no significant difference was found between the PTT obtained from these two approaches. This implies that the changes in PTT are not induced by the complete occlusion of the brachial artery, which only happens in case of the deflation approach. Rather, the amount of PTT changes mainly depends on the applied cuff pressure.

This observation may not hold if the inflation, deflation or occlusion period is extended, as previous study also reported that smooth muscle relaxation would appear in postocclusive reactive hyperemia, resulting in vasodilatation and further altered the arterial properties. The results of the previous study indicated that smooth muscle relaxation would increase brachial artery compliance and decreases PWV [98].

The analysis of PTT at different cuff pressures during inflation and deflation offers complementary information to factors that could have influence PTT measurements, and may also help in assessing individual arterial properties for calibration. Yet it still involves the use of a cuff-based BP device and thus another factor, i.e. hydrostatic pressure, which may be used to develop a more convenient calibration procedure.

3.2 The Effects of Hydrostatic Pressure

There is another pressure variation within the body which occurs when one part of the body is at a different elevation than another. This is called hydrostatic pressure (P_H), which arises because of the gravitational potential energy of the blood. Essentially, blood that is at a higher elevation has greater potential energy. The hydrostatic pressure difference due to a difference in height is given by $\Delta P_H = \rho g \Delta h$.

Gundersen reported a reduction of the digital systolic blood pressure (SBP) greater than the hydrostatic pressure change during hand elevation [99]. Foo *et al.* reported a significant increase in PTT calculated from finger photoplethysmogram (PPG) when the test arm was vertically raised [100]. However, little is known about the changes in PTT and its correlation with corresponding peripheral BP during the process of arm elevation. The objective of this study is to quantitatively examine the PTT and BP changes as well as the correlation coefficients between PTT and radial BP at discrete vertical wrist positions above heart level.

3.2.1 Experimental protocol

Pre-experiment Test

For each subject BP was simultaneously measured from left upper arm and right wrist for three times at rest status using automatic BP devices (Omron HEM-907 and National EW280, respectively). The difference between the mean BP readings from the two devices was considered as bias, and was removed from the radial BP readings obtained later during the arm elevating session for each individual.

Two reflective PPG sensors (EVERLIGHT, PT11-21C-L41-TR8 and IR11-21C) named PPG-1 and PPG-2 having the same circuit design, were made with different configurations. PPG-1 was located inside a ring sensor with an adjustable contact force, which was measured by a force sensor (MSIsensors FC21). PPG-2 was located inside a light band. These two sensors were fixed around the right index and ring fingertips respectively during the whole experiment.

Experiment Protocol

Eleven healthy volunteers aged from 20 to 53 including 4 females were recruited in the experiment. Subjects were seated upright and their right arms were kept constantly at the heart level during the whole experiment. They were requested to stretch out their right (test) arm unbent to different vertical wrist positions above heart level (h) without support. The h was set to be 0, 15, 30, 45 and 60 cm in a randomized sequence, where the test arm was held for 15s for ECG and PPG recordings. One schematic show of experimental setup is given in Fig. 3.5.

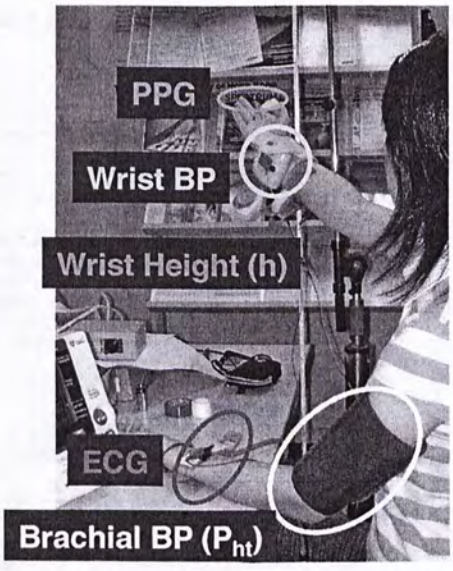

Fig. 3.5: Experimental setup for this study (subject was holding her right wrist at h=30 cm).

After this procedure, subjects were instructed to stretch the test arm to the five wrist positions again. BP readings from the test wrist (right wrist) and the stable arm (left arm) were simultaneously measured using the mentioned automatic devices, while their arms were maintained at each h. One minute was allowed in between each two BP measurements.

PTT was measured as the time interval from the peak of the ECG R wave to the upstroke of the PPG pulse in the same cardiac circle. Data were presented as mean±standard deviation (SD). The paired student's t-Test was used to examine the difference and $p<0.05$ was regarded as statistically significant.

3.2.2 Analysis for the Effects of Hydrostatic Pressure on PTT

For all the subjects, the mean arterial blood pressure (MBP) was calculated from $MBP = DBP + (SBP - DBP)/3$. One trial of PTT at h = 45 cm, two trials of PTT and one set of radial BP at h = 60 cm were absent due to the measurement failures.

As shown in Fig. 3.6, the radial MBP from the test arm reduced, while PTT values from PPG-1 and PPG-2, named PTT-1 and PTT-2, increased with the ascending h. The radial MBP calculated by $MBP_0 - \rho gh$ was illustrated in Fig. 3.6 (a) as a dashed line. The contact force between PPG-1 and the test index fingertip (F_{ext}) was

normalized by that at $h = 0$ cm for each subject and shown in Fig. 3.6 (c).

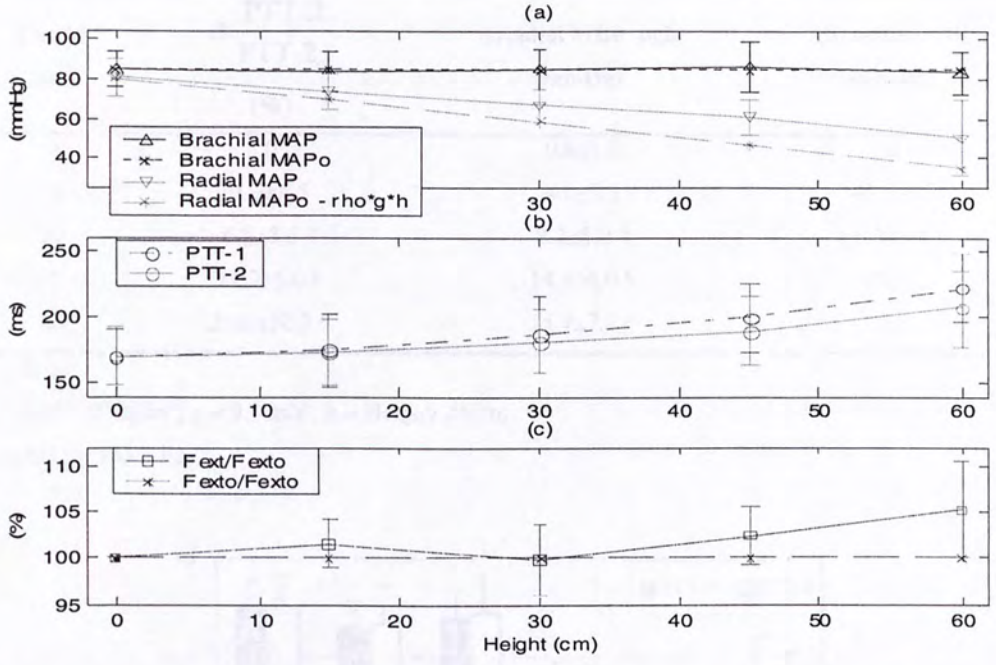

Fig. 3.6: The mean values (mean±SD) of (a) Measured brachial and radial MBP, (b) PTT from two PPG sensors, and (c) Normalized F_{ext} for all the individuals at different vertical wrist positions [101].

Moreover, as presented in Table 3.1, the heart pressure denoted by the brachial MBP remained stable, while the changes in the measured radial MBP were somewhat less than ρgh at each h. On the other hand, the normalized PTT-2 changes showed that PTT values at $h \geqslant 30$ cm were significantly different from those at heart level ($p<0.05$).

It was indicated in Table 3.2 that for most subjects, both PTT-2 and the radial BP were almost linearly correlated with h; During the hand elevation process, PTT-2 and radial BP were significantly correlated ($p<0.05$) for each individual. PTT-1 followed a similar trend as PTT-2, which is shown in Fig. 3.7.

Table 3.1: Percentage Changes of PTT-2, Difference Between Measured Radial MBP Change and ρgh, and Brachial MBP Changes from Heart Level at Different Wrist Positions [101].

Height (cm)	$\Delta\frac{\text{PTT-2}}{\text{PTT-2}_0}$ (%)	ΔRadial MBP -ρgh (mmHg)	ΔBrachial MBP (mmHg)
0	0	-0.8±1.3	0
15	1.7±4.5	-4.0±5.3	-0.7±3.5
30	6.6±3.5 *	-8.2±5.0 *	0.3±3.8
45	11.2±5.0 *	-14.4±4.0 *	1.5±5.1
60	21.8±10.3 *	-15.9±7.9 *	-1.5±3.6

* $p<0.05$

$\rho = 1.05*10^3$ kg/m^3, g = 9.8 m/s^2, h = Height/100 m,

1 mmHg = 133.3 Pa.

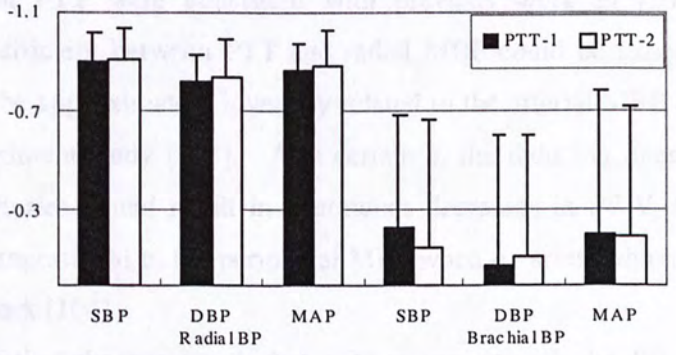

Fig. 3.7: Averaged individual correlation coefficients between PTT and radial BP as well as between PTT and brachial BP of all the subjects [101].

Table 3.2: Averaged Correlation Coefficients Between Height and PTT-2, height and BP, AND between PTT and BP of All the Subjects [101].

r	Height	PTT-2
PTT-2	0.94±0.10 [1]	N/A
Radial MBP	-0.97±0.02 [0]	-0.88±0.14 [3]
Radial SBP	-0.96±0.04 [1]	-0.91±0.13 [2]
Radial DBP	-0.95±0.03 [1]	-0.84±0.15 [4]

The superscript represents the number of subjects with $p>0.05$.

3.2.3 Section Discussions

In the present study, it is demonstrated that the MBP at heart level kept roughly constant, while the radial MBP gradually reduced with a raising wrist position. Similar phenomena were also found in other studies [99, 100]. The somewhat less reduced radial MBP compared with theoretical hydrostatic pressure change during limb elevation was reported by previous work in popliteal arterial pressure [102]. This might be attributed to several factors such as the transfer of kinetic energy that was ignored in our current calculations, the autoregulation mechanism in skeletal muscle, and the holding of the arm without any support while measuring the BP.

On the other hand, PTT progressively increased with the rising h and was significantly longer when measured at h = 30 cm than that at heart level. The effects of position on PTT were consistent with previous work in [100]. The high correlation coefficient between PTT and radial MBP could be expected if PWV is considered to be approximately inversely related to the arterial MBP as supported by previous experiment study [103]. At a certain h, the reducing internal MBP along the transfer arteries would result in continuous decreases in PWV, and PTT would therefore be proportional to the peripheral MBP when h varies, which was elaborated in our other work [104].

Another interesting phenomenon is that, with an ascending h, the differences between PTT-1 and PTT-2, i.e. PTT_{diff} in an increasing manner was illustrated in Fig. 3.6 (b). At the same time, a raising trend of normalized F_{ext} could also be observed as shown in Fig. 3.6 (c). The PTT_{diff} at the same h might be attributed to the unequal contact force that applied on the test index and ring fingertips, since it was reported that an increase of digital P_{tm} would result in a prolonged PTT [94]. This is also supported by the occurrence of the increasing trend of PTT_{diff} and F_{ext} observed with larger h in this study.

The increased PTT and decreased radial BP with the rising h, as well as high correlation coefficients between the two were observed during the hand elevation process indicates the potential of using the PTT-based approach to continuously monitor peripheral BP, while allowing the concerned limb positioned at different levels from the heart. This would be helpful for clinical applications such as hand surgeries and studies of reactive hyperemia.

3.2.4 Section Summary

In this chapter, the results of two experiments study the effects of two components of transmural pressure (i.e. P_E and P_H) on PTT that is used in this thesis for BP measurement. The two directions could be further investigated to build up physiological models for calibration and estimation processes (later a calibration method utilizing the cuff deflation process has been proposed in [97], the use of cuff inflation/deflation per se limits its application on cuffless calibration approaches for BP estimation. I selected the direction which involves hydrostatic pressure changes. Through modeling the effects of PTT under the arm elevation induced P_H changes, a bio-physical model for cuffless calibration method will be proposed in the next chapter.

CHAPTER 4

Modeling the Effect of Hydrostatic Pressure on PTT for A Calibration Method

As described in chapter 3, PTT increases with the hydrostatic pressure during arm elevation. The objective of this chapter is to model PTT under the effects of hydrostatic pressure during the arm elevation process, and propose a model-based hydrostatic calibration method for BP estimation.

4.1 Current Status of Hydrostatic Calibration Approaches

Limited work has been done to utilize hydrostatic pressures for the purpose of calibration [12, 81, 90]. In [81] the PTT is assumed as linearly related to BP, while this linear relationship has been shown on certain BP ranges. In [90] a series of different postures (supine, sitting or standing) and the resulted changes in hydrostatic pressure and PTT are used to estimate BP. In their work the slope of PTT-P_H cureve was directly used as the slope in the linear equation describing arterial BP and PTT. However, the approximation of PTT-P_H relationship for PTT-BP relationship is somehow lack of theoretical foundation and may need further verifications. Both [81] and [90] need an initial use of BP from a cuff-based device to calculate the model parameters. The work done in [12] provides a table of mapping coefficients to relate PTT and MBP cufflessly, based on the hydrostatic calibration equation utilizing different a V-P model Nevertheless, this method only works over limited ranges of a coefficient of the model and is not only for MBP prediction.

In this chapter a method targets to measure BP (more specifically to measure SBP) using a calibration approach based on a model describing the PTT-P_H relationship is

to be proposed. Comparing with the previous studies, the newly proposed method utilizes simple arm movements that are easy to carry out and aims to monitoring the clinically valuable parameters.

4.2. Modeling Pulse Transit Time under the Effects of Hydrostatic Pressure for A Hydrostatic Calibration Method:

4.2.1 Basic BP-PTT model

Started from the famous Bramwell-Hill equation which describes pressure pulse transmission in arteries based on bulk modulus:

$$PWV = \sqrt{\frac{V}{\rho}\frac{dP}{dV}} \tag{2.3}$$

It is noticed that equation (2.3) if the right side of equation can be written as a function of only the BP and some other measurable parameters, a theoretic model for BP and PTT would be obtained.

4.2.2 V-P relationship Represented by a Sigmoid Curve

In this study, I used the simplest representations of the arterial volume-pressure relationship, that is the sigmoid curve also mentioned in [105]:

$$V = \frac{a}{1+\exp(-bP_{Tr})} \tag{4.1}$$

where a and b are related to the properties of the artery and P_{Tt} (transmural BP).
The derivative of V in terms of P_{Tr} was calculated:

$$\frac{dV}{dP} = \frac{a \cdot b \cdot \exp(-b \cdot P_{Tr})}{[1+\exp(-b \cdot P_{Tr})]^2} \tag{4.2}$$

By substituting (4.1) and its derivative (4.2) into (2.3), and understanding that P_H and P_E have no effect if no ΔP_H or ΔP_E is to be intentionally introduced, we have:

$$BP = P_I = \frac{1}{b}\ln(\frac{L^2\rho b}{PTT^2} - 1) \tag{4.3}$$

and its approximation:

$$BP \approx -\frac{2}{b}\ln(PTT)+\frac{1}{b}\ln(L^2\rho b) \tag{4.4}$$

4.2.3 Relating PTT with Hydrostatic Pressure

According to (4.3), the time (Δt) needed for a pressure pulse to travel through a small segment of an artery with length Δl is found to be:

$$\Delta t = \frac{\Delta l}{PWV_t} = \sqrt{\frac{\rho b}{1+\exp(bP_t)}}\,\Delta l \tag{4.5}$$

To build up the relationship between PTT and hydrostatic pressure, subjects are asked to elevate their hands at an angle (θ) with respect to the horizontal plane. Integrating for the complete artery segments of arm length L gives:

$$PTT = \int_0^T dt = \int_0^L \sqrt{\frac{\rho b}{\exp(b\cdot P_{tr})+1}}\,dl \tag{4.6}$$

where P_{tr} is the internal blood pressure at any point along the artery. Through this process no external forces are applied to subjects, the contact force between PPG sensor and fingertip is kept as a fixed value by using carefully selected sensors, and the changes in blood flow velocity are negligible. Under these conditions P_{tr} at any point along the artery differs from P_{tr} at heart level (P_I) by corresponding hydrostatic pressure (P_h):

$$P_t = P_I - P_h \quad \text{and}$$

$$P_h = \rho g l\cdot\sin\theta = \rho g h \tag{4.7}$$

After substituting (4.7) into (4.6) we finally get:

$$PTT = \begin{cases} \dfrac{L\sqrt{\rho b}}{\sqrt{1+\exp(bP_I)}} & ;\quad H=0 \\ \dfrac{2L}{gH\sqrt{\rho b}}\ln\left|\dfrac{\sqrt{\exp[b(P_I-P_H)]+\exp(-bP_H)}-\sqrt{\exp(-bP_H)}}{\sqrt{\exp[b(P_I-P_H)]+1}-1}\right| & ;\quad H\neq 0 \end{cases} \tag{4.8}$$

where P_I is the internal BP at heart level, $H=L\cdot\sin\theta$ is the vertical distance between the peripheral site and heart level. $P_H=\rho gH$ is the hydrostatic component corresponding to peripheral BP that differs from P_I. Fig. 4.1 shows the difference in BP at heart level and periphery for an artery inside an elevated limb. Fig. 4.2 shows the simulated ΔPTT-H curve simulated based on equation (4.8), given L=70 cm. It can be observed in Fig. 4.2 that the different percentage changes of PTT for positive and

negative H are related to b: the larger the b, the more unsymmetrical the ΔPTT for positive and negative Hs. It should be noticed that the ΔPTT-H curve has the same pattern under any heart pressure readings, and is only subject to b and L.

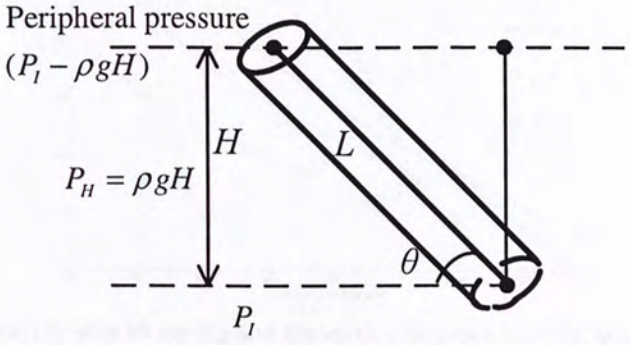

Fig. 4.1: The blood pressure at heart level and periphery for an artery that is being held at an angle with respect to the horizontal plane.

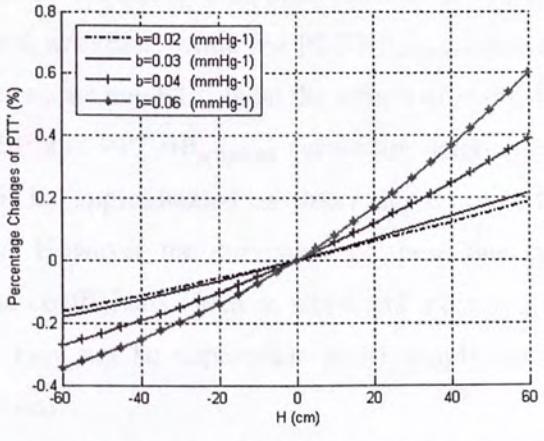

Fig. 4.2: Percentage changes of PTT over H from -60 to 60 cm, given L=70 cm.

Fig. 4.3 shows the theoretically simulated PTT-BP as well as PTT-$BP_{peripheral}$ curves with L=70 cm. The theoretical PTT-$BP_{peripheral}$ curves are plotted over H=-60 to H=60 cm, assuming BP≡90 mmHg and a vertical distance between heart level and shoulder level (H_{sh-h}) equals to 10 cm.

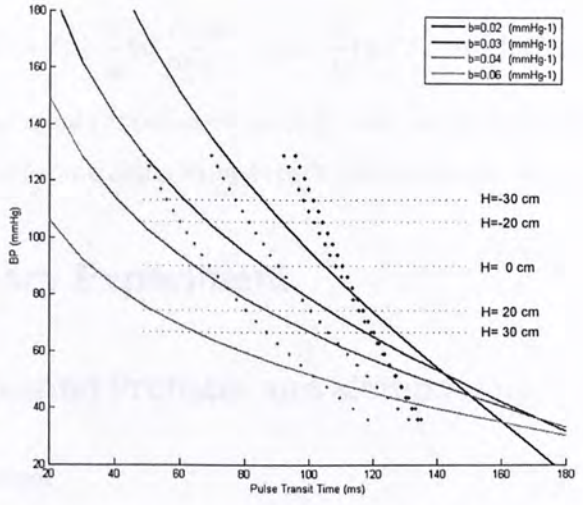

Fig. 4.3: MBP at heart level is 90 mmHg and the vertical distance between heart and shoulder is assumed as 10 cm.

The PTT-BP curve describes changes in brachial arterial pressure and PTT under conditions like physical activities, while the PTT-$BP_{peripheral}$ curve describes changes in peripheral arterial pressure and PTT under the effects of hydrostatic pressure. The shapes of both PTT-BP and PTT-$BP_{peripheral}$ curves are determined by the individual coefficient b and can be approximated as linear curves over PTT within normal physiological ranges. However the curvatures of these two curves are different, which implies that the coefficients (such as slope and intercept) of simplified linear PTT-$BP_{peripheral}$ curve may not be appropriate to be simply used in linear PTT-BP models for BP estimation.

4.2.4 Implementing the Hydrostatic Calibration Method for BP Estimation

As expressed in equation (4.8), PTT is a function of H given a set of subject-dependent coefficients $\{L, b\}$ and constants $\{\rho, g\}$ at a specific initial internal BP (P_I). To implement it, the calibration procedure is to calculate b given other parameters measured from subjects.

On the other hand, given a set of coefficients and constants $\{L, b, \rho, g\}$, P_I can be expressed in terms of measured PTT while the subject maintains his/her hand at the heart level (i.e. H =0 cm) as shown in equation (4.3) and (4.4):

$$BP = P_t = \frac{1}{b}\ln(\frac{L^2\rho b}{PTT^2} - 1) \approx -\frac{2}{b}\ln(PTT) + \frac{1}{b}\ln(L^2\rho b)$$

A preliminary experiment (experiment week 0) was conducted to test the performance of the proposed hydrostatic calibration as presented in section 4.3.

4.3. Preliminary Experiment

4.3.1. Experimental Protocol and Methodology

Experimental Protocol

In order to test the method presented in 4.2.4, eight volunteers aged 23 to 36 which included 3 females were recruited in an experiment which contained a session for calibration and a session for estimation. None of the subjects reported any chronic cardiovascular diseases. All subjects were instructed about the study procedure and gave their informed consent to participate in the study. Subjects were seated upright and their left arms were held at heart level throughout the experiment. Fig.4.4 showed the set up of this experiment.

In the calibration session, the length of each subject's right arm L was measured from shoulder (acromion) to the fingertip of index finger. Subjects were then asked to stretch out their right arms unbent and lift their wrists to different heights (H) with respect to their shoulders. Following the marks on a board placed next to the subjects, they were asked to raise their wrists to H = -30, -20, 0, 20 and 30 cm in a randomized order. The angle of elevation was also monitored by an accelerometer. ECG and PPG signals were recorded for 20s from the right wrist while it was held at each height level. Immediately after signal recording, brachial BP of the left arm and radial BP of the right wrist were measured simultaneously by two automatic BP devices (Omron HEM-907 and HEM-642-HK). Subjects were allowed to rest for one minute in between two heights. The H later used for calculation is an average of the height monitored by accelerometer and the height by the set wrist height (e.g. 0, ±20 and ±30 cm) plus the accelerometer monitored wrist-finger height.

In the estimation session, three BP measurements and two signal recordings were obtained from each subject. Afterwards, subjects were asked to ride on an ergometer for four minutes after which three BP measurements and two signal recordings were made. The session after exercise was repeated once and therefore in total six sets of

signal recordings were obtained for each subject. A schematic figure showing the experimental protocol is shown in Fig. 4.5.

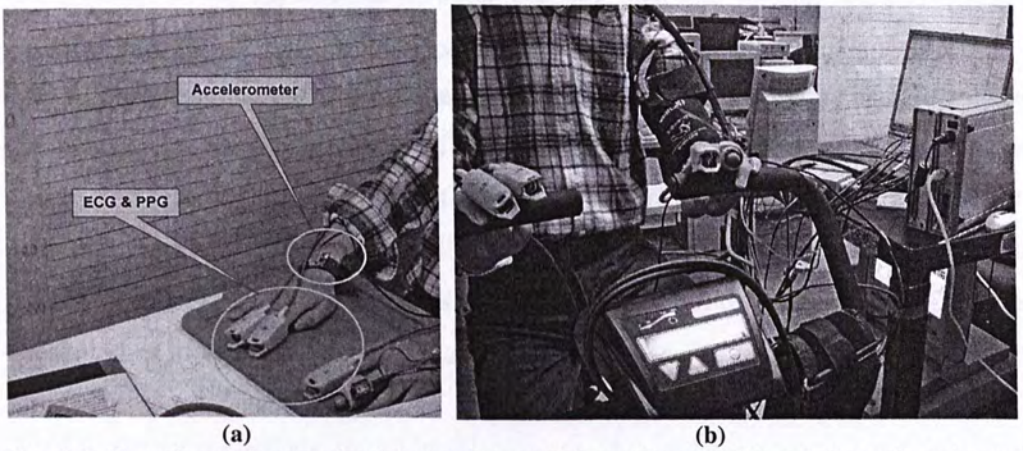

(a) (b)

Fig. 4.4: Experimental setup for (a) signal recording session and (b) exercise and post-exercise sessions on an ergometer.

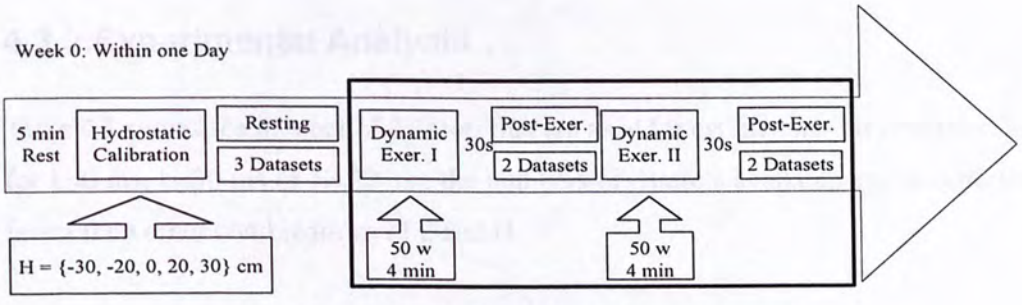

Fig. 4.5: A schematic figure for experimental protocol.

Methodology

In this preliminary experiment, the model presented as equation (4.8) and (4.3) are modified as follows:

$$PTT = \begin{cases} \dfrac{L\sqrt{\rho b}}{\sqrt{1+\exp(bP_1)}} + k & ; H=0 \\ \dfrac{2L}{\sqrt{\rho b}gh} \ln\left| \dfrac{\sqrt{\exp[b(P_1-P_H)]+\exp(-bP_H)} - \sqrt{\exp(-bP_H)}}{\sqrt{\exp[b(P_1-P_H)]+1}-1} \right| + k & ; H \neq 0 \end{cases} \qquad (4.8\text{-}1)'$$

$$SBP = \frac{1}{b} \ln\left(\frac{L^2 \rho b}{(PTT-k)^2} - 1 \right) \qquad (4.3\text{-}1)'$$

where the individual-dependent coefficient b is calibrated from (4.8-1) and then

substituted into (4.3-1) for estimation. The coefficient b is a measure of the arterial elasticity. In this study, a constant k was introduced to be subtracted from PTT. k was chosen to be {0, 30, 40, 50, 60, 70, 80} ms. Considering the physiological meaning of PTT, all datasets with k>PTT were not be included for calculation.
The PTT collected at each H and the corresponding brachial BP were used to calibrate the coefficient b from equation (4.8). After calibration, each set of {L, b} were substituted into the simplified equation (4.4) for estimating SBP. Reference SBP for each signal recording was obtained by averaging the SBP measured before and after. The estimation error was defined as the estimated BP minus the reference. Data were presented as mean±standard deviation (SD).

4.3.2. Experimental Analysis

Table 4.1 shows the number of datasets that are used for estimation. It is noticed that for k=0 ms, k=30 ms or H=30 cm, the numbers of datasets available are considerably fewer than other combinations of k and H.

Table 4.1: Number of Datasets Used for Overall SBP Estimation

k (ms) \ H (cm)	-30	-20	0	20	30
0	12	12	12	12	5
30	34	40	34	28	24
40	46	46	40	40	30
50	46	46	46	46	30
60	45	45	45	45	30
70	40	40	43	43	30
80	40	40	40	41	36

For combinations of k and H with more than 20 datasets available, the mean and SD of estimation errors resulted from each combination are normalized by those obtained at H=-30 cm and presented in Fig. 4.6.

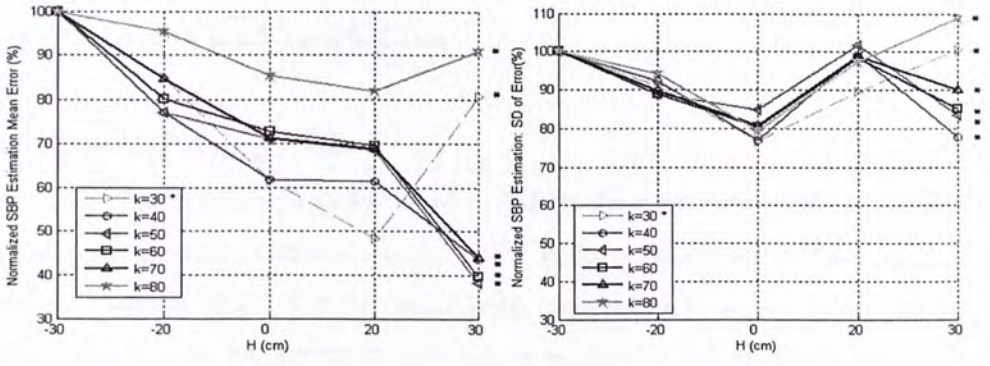

(a) (b)

Fig. 4.6. Normalized SBP estimation results from all the datasets of 8 subjects: (a) Mean, and (b) SD of error for different k (ms) and wrist height H (cm).

*** Available datasets less than 40**

Fig. 4.7 shows the changes of radial SBP from that measured at H=0 cm for each individual as well as the mean and SD of these changes for all subjects. The theoretical changes (i.e. $P_h=\rho gh$) are also presented in Fig. 4.7. It is noticed that the changes in radial SBP vary across subjects for the same H; however the mean changes in radial SBP for all subjects agree well with the theoretically predicted values.

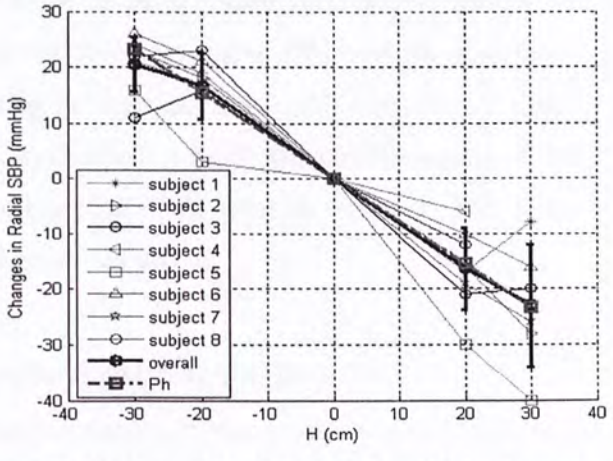

Fig.4.7: Changes in radial SBP for each individual (thin solid lines), mean and SD of radial SBP changes for all subjects (thick solid line) and P_h (thick dashed line) during calibration session.

4.4. Section Discussions

Estimate SBP using PTT

Noticed is that in equation (4.4) and (4.8) 'BP' is the mean arterial pressure, which is not used for clinical examination, and 'PTT' is the arterial component (PTT') which does not include PEP. On the other hand, my object is to develop a calibration method that can be implemented with simple equipment and satisfy clinical demand. Thus the parameters that can be used to measure systolic and diastolic blood pressure and are easy to measure would be preferred.

The study done by Payne *et al.* [106] supports the idea of using the ECG initiated PTT to estimate SBP. In their work, it is mentioned that PTT' is more correlated to MBP and DBP compared with PTT initialed from ECG, while PTT initialed from ECG is highly correlated with SBP, even under the effects of several cardiovascular drugs. This is possibly because the two components of PTT, PEP and the time it takes the pressure pulse travel from aorta to periphery (PTT'), are both inversely related to SBP. Under the situation e.g. exercise when SBP is greatly increased, there often induces a significantly increasing in pulse transit time within arteries since the arterial wall becomes rigid and thus a decreasing in PTT'; on the other hand, exercise induces a significant increasing in heart rate due to the regulation of central never system, and the acceleration of heart rate is accompanied by shortening of PEP. Therefore in this study, the ECG initiated PTT is used to estimate SBP with the calibration and estimation models presented above.

Discussions for the Experimental Results

From the experimental results of this study, it is noticed that the mean and SD of estimation errors are related to two factors: the constant k and the calibration height H. We then grouped all the datasets with the same H to exam the affects of k on BP estimation, and vice versa.

As shown in Fig. 4.6, the mean and SD of estimation errors of the hydrostatic calibration approach differ slightly to moderately over $40 \leq k \leq 70$ ms at any given H. It should be mentioned that in this study, k is a time interval subtracted from the ECG initiated PTT and is different from the concept of PEP. In this study, we adjusted PTT by subtracting a constant k from it. The estimation results over $40 \leq k \leq 70$ ms

vary little, implying the potential of using the adjusted PTT in the hydrostatic calibration model for estimating SBP. From Fig. 4.6 (a) and Table 4.1, it is also noticed that the extreme values of k (0, 30 and 80 ms) should be avoided, since they may resulted in unrealistically short PTT and less available datasets after the adjustment.

Nevertheless, the mean and SD of estimation errors differ with H for any k between 40 and 70 ms. A decreasing trend of the estimation mean errors with the calibration height is found for $40 \leq k \leq 70$ ms while no such trend can be observed for the SD of estimation errors. The variations of estimation results at different calibration Hs may relate to the different responses in peripheral BP and PTT against the hydrostatic pressures introduced by hand elevation. We noticed from Fig. 4.7 that although from H=0 cm to any other particular H there exist inter-subject differences, the mean changes in radial SBP of all subjects are close to the theoretical values (i.e. changes in P_h with H), which are symmetrical about H=0 cm. On the other hand, the increase of PTT with H is more remarkable for H>0 cm than that for H<0 cm as reported in [107]. Therefore when $\{P_l, P_H, \text{PTT}\}$ are substituted into equation (4.8)' for calibration, the same magnitude of error in PTT measured at H<0 cm compared with that measured at H>0 cm may result in a larger variation in b. Nevertheless, it may also be possible that the measurement errors in BP, PTT and finger heights appeared at $H \neq 0$ cm contribute to the differences in estimation results across Hs.

4.5. A Novel Implementation Algorithm of Hydrostatic Calibration Method for Cuffless BP Estimation

It is noticed that in the modeling process that an initial BP (P_l) is still needed. In [12] a PTT-MBP mapping algorithm was developed based on simulation results that the ratio of PTT changes over arm length is slightly changed with b values over special range but is correlated to MBP [108]. However, as I will show in this study, the b values obtained from experimental results are somehow out of the range of b required in [12]. Moreover, the fixed coefficients for mapping PTT to MBP are still challengeable before they are improved to be applicable for most subjects. Yet is it still necessary to explore the way to utilize the proposed calibration model for BP estimation.

An interesting point noticed is that, although equation (4.8) is the integrated format of unit models described as (4.3) arranging in a tilted line, these two equations are describing different aspects of information reflected by PTT. Thus I substitute the simplified equation (4.4) into (4.8) and get:

$$PTT_2 = \frac{2L}{gH\sqrt{\rho b}} \ln \left| \frac{\sqrt{\exp[\ln(\frac{L^2 \rho b}{PTT_1^2}) - bP_H)] + \exp(-bP_H)} - \sqrt{\exp(-bP_H)}}{\sqrt{\exp[\ln(\frac{L^2 \rho b}{PTT_1^2}) - bP_H)] + 1} - 1} \right|; \quad H \neq 0 \qquad (4.9)$$

where PTT_1 and PTT_2 are PTTs obtained at different heights for calibration. Through modeling PTT under the effects of the induced hydrostatic pressures, a modified mathematical equation is presented as equation (4.9) in which the individual coefficient b can be cufflessly calibrated from the relationship between PTTs and H given a set of $\{L, H, \rho, g\}$. Later on the parameters $\{L, \rho, b\}$ are substituted into equation (4.4) for BP estimation of the same subject. Two experiments with the same protocol (experiment week I and II) were conducted to test the performance of this modified hydrostatic calibration and the results are presented in chapter 5.

4.6. Section Summary

In this chapter a bio-physical model-based hydrostatic calibration approach is derived. A preliminary experiment was done to test its performance and the experimental results are analyzed and discussed. Furthermore based on this hydrostatic calibration model a novel implementation algorithm is proposed with which the individual coefficient b can be cufflessly calibrated.

CHAPTER 5

Experimental Studies for the Hydrostatic Calibration Approach

As discussed in chapter 4, the proposed model for hydrostatic calibration method has been modified so that the ECG initiated PTT can be used. In this chapter two experiments were carried out in order to verify this modified hydrostatic calibration approach.

5.1 Experimental Analysis

5.1.1 Experimental Protocol

Two experiments were carried out following the same experimental protocol. The 1st experiment (week I) included 15 subjects (7 of them are female) aged from 23 to 37 years. Four subjects appeared in the 2nd experiment (week II). Experiment week II included 15 subjects (6 of them are female) aged from 25 to 34 years. None of the subjects reported any chronic cardiovascular diseases. All subjects were instructed about the study procedure and gave their informed consent to participate in the study. Table 5.1 shows information of the numbers participated in both experiment week I and week II. Fig. 5.2 (a) shows the ECG and PPG sensors used in these two experiments.

Table 5.1: Information of the Subjects Participated in Experiment Week I and II

Number of subjects	**30 (4 are duplicated)**
Age	**23~37 years old**
Gender	**13 Females and 17 Males**
Arm length	**70 ± 5 (cm)**

In the very beginning, subjects were seated and their brachial BP from left arm was measured twice. For the first time subjects' left arms were put on a table, maintaining the cuff at their heart level. For the second time subjects were asked to hold their whole left arms unbent horizontally. Subjects were then asked to seat upright and hold their left arms at heart level throughout the experiment. In the calibration session, the length of each subject's right arm L was measured from shoulder (acromion) to the fingertip of index finger. Subjects were then asked to stretch out their right arms unbent and lift their wrists to different heights (H) with respect to their shoulders. Following the marks on a board placed next to the subjects, they were asked to raise their wrists to H = -30, -20, 0, 20 and 30 cm in a randomized order. The angle of elevation was also monitored by an accelerometer. ECG and PPG signals were recorded for 20s from the right wrist while it was held at each height level. Immediately after signal recording, brachial BP of the left arm and radial BP of the right wrist were measured simultaneously. Subjects were allowed to rest for one minute in between two heights.

In the estimation session, four brachial BP measurements and three signal recordings were obtained from each subject during resting status. Afterwards, subjects were asked to run on a treadmill for 3 minutes (10 km/hr) after which four brachial BP measurements and three signal recordings were made immediately.

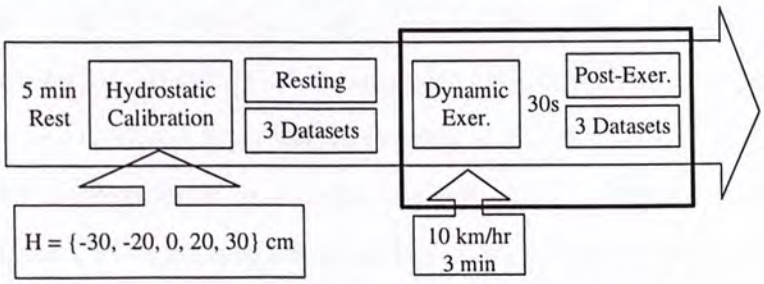

Fig. 5.1: A schematic figure showing the experimental procedures.

Reference SBP for each signal recording was obtained by averaging the SBP measured before and after. In these two experiments, a mercury column and an automatic BP device (Omron HEM-907) were connected by a Y-shape tube as shown in Fig. 5.2 (b). Therefore the nurse reading from the stethoscope and reading from BP device could be obtained simultaneously and then averaged. The radial pressure was measured by another wrist type automatic BP device (HEM-642-HK).

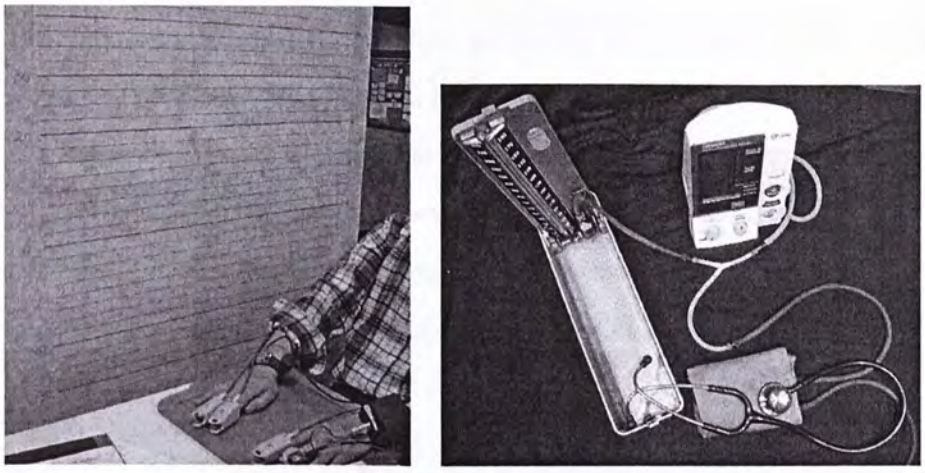

Fig. 5.2: (a) Finger clips with ECG, PPG sensors and accelerometer sensor on the right wrist and (b) Stethoscope and automatic BP device connected by a Y-tube.

ECG, PPG and the signal from accelerometer were recorded at a sampling rate of 1000Hz during the process. In total 5 sets of signal recordings were obtained during calibration session and 6 sets of signal recordings were obtained during estimation session for each subject.

5.1.2 Methodology

The calculations of PTT and of corresponding reference BP are shown in Fig. 5. 3. The experimental results presented in this chapter are mainly focused on testing the performance of calibration approaches described in equation (4.9). If PTT_1 is from $H=0$ and PTT_2 is from $H\neq0$, it is defined as hydrostatic calibration method I. For this method, the PTT from H=0 cm is defined as PTT_0, while PTTs from other four heights are defined as PTT_h. PTT_0 is then paired with each of the four PTT_h to calibrate b according to equation (4.9).

On the other hand, if PTT_1 is from the resting process during which subject's hand is held at heart level and PTT_2 is obtained from the arm elevation process, it is defined as hydrostatic calibration method II. For this method, PTT from the 1st dataset in resting session is defined as PTT_{r1} and PTTs collected at five heights are defined as PTT_h. PTT_{r1} is then paired with each of the five PTT_h to calibrate the coefficient b from equation (4.9).

After calibration, each set of {L, b} were substituted into equation (4.4) to estimate SBP for the rest datasets. The brachial BP corresponding to the reference PTT (PTT_0 or PTT_{rl}) defined as BP_0 or BP_{rl} was further used to calculate the pressure bias (P_{bias}) between the calculated BP and reference BP for the calibration point. P_{bias} was further corrected during the BP estimations. The estimation error was defined as the estimated BP minus the reference. Data were presented as mean±standard deviation (SD).

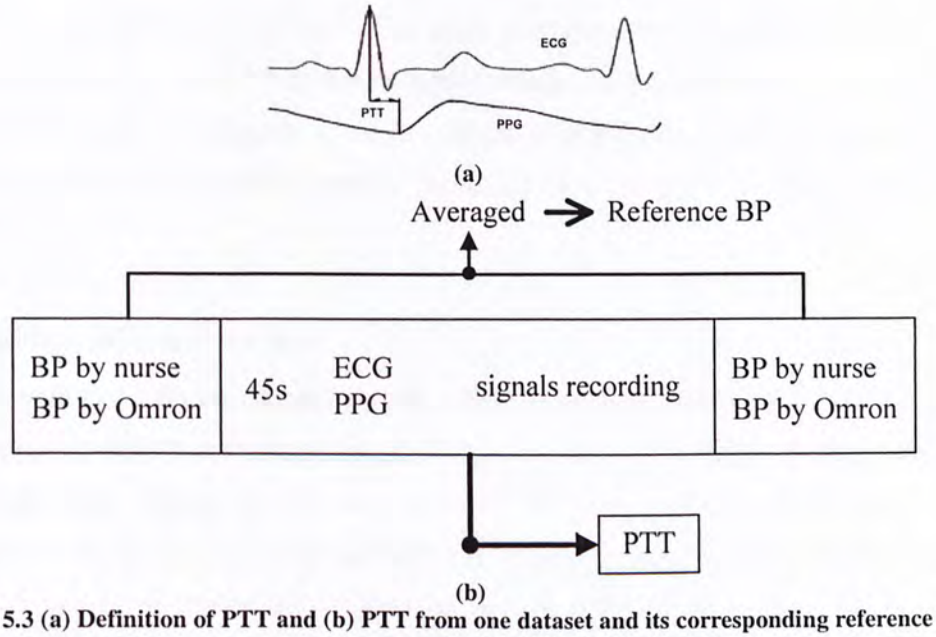

Fig. 5.3 (a) Definition of PTT and (b) PTT from one dataset and its corresponding reference BP.

5.1.3 Preparations

Among the 150 datasets of 30 subjects for calibration session, all 5 trials of subject 1.9 (i.e. the 9th subject in experiment week I) are removed due to the noisy ECG signals; all 5 trials of subject 1.11 are removed because the amplitude of PPG signal of this subject is too small to detect the feature points. For other calibration trials, it happens that the amplitude of PPG signal diminished due to the increased calibration height (H) and therefore reduced peripheral BP. It is difficult to identify the feature point on PPG signal with such small amplitude and these datasets (i.e. for H=20 cm: subjects 1.14, 1.15, 2.9 and 2.11; for H=30 cm: subjects 1.14, 1.15, 2.3 and 2.11) are thus removed. Totally 132 trials from 28 subjects are available for the calibration session. An example of noisy PPG signals is given in Fig. 5.4.

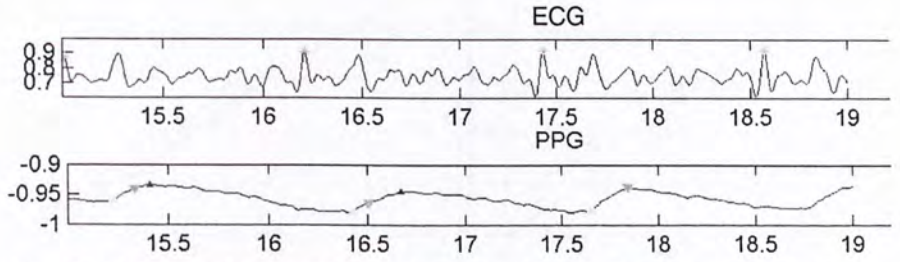

Fig. 5.4: Example of noisy PPG signal: ECG and PPG of subject 1.15 at H=20 cm.

Among the 180 datasets collected for BP estimation, all 6 trials of subject 1.9 and 1.11 are removed because of the very noisy ECG and small PPG amplitude, respectively. Besides, record of the 1st trial during post-exercise process of subject 2.1 is missed. Therefore totally 167 datasets from 28 subjects who attended experiment week I and II (4 subjects in experiment week I were repeated in week II) are used for BP estimation.

Reference Blood Pressures

As mentioned above, brachial BP were measured simultaneously from a sphygmomanometer and an automatic BP device, and the average of these two BP readings were averaged and used as the reference pressure for a single BP measurement. Fig. 5.5 shows the overall BP readings from the sphygmomanometer and the automatic device for all datasets used in BP estimation from 28 subjects. Overall, the BP readings from automatic BP device differ from the readings from sphygmomanometer (nurse readings) by -2.3±4.4 mmHg and -4.3±3.6 mmHg for SBP and DBP, respectively.

The brachial BP readings decrease when subjects hold their arms horizontally comparing with remaining their arms at heart level. Overall the mean BP readings measured at shoulder level are lower than BP measured at heart level by 5.8±4.7 mmHg for SBP and 4.6±3.5 mmHg for MBP.

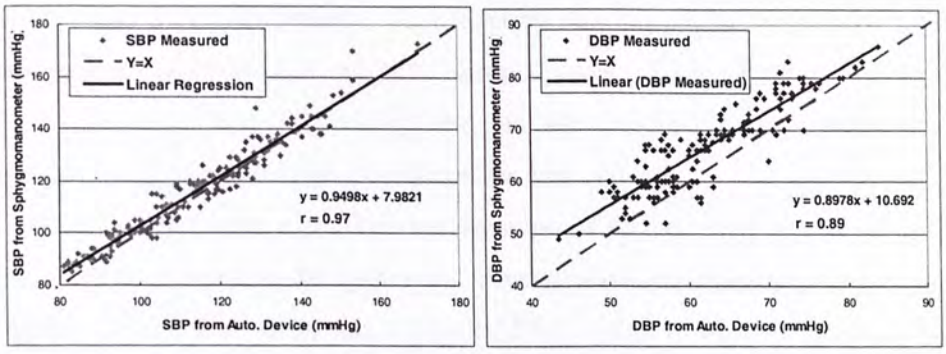

(a) (b)

Fig. 5.5: (a) SBP and (b) DBP readings from a stethoscope and an automatic BP device (Auto. Device) connected by a Y-tube for all 28 subjects attended in experiment week I and II.

Blood Pressure Dynamic Ranges

The overall BP dynamic ranges (defined as the maximum minus the minimum) are 32±8 mmHg for SBP and 5±3 mmHg for DBP. Fig. 5.6 shows the number of subjects with different BP ranges and it is noticed that SBP experienced large dynamic changes after the exercise while DBP experienced only slight changes.

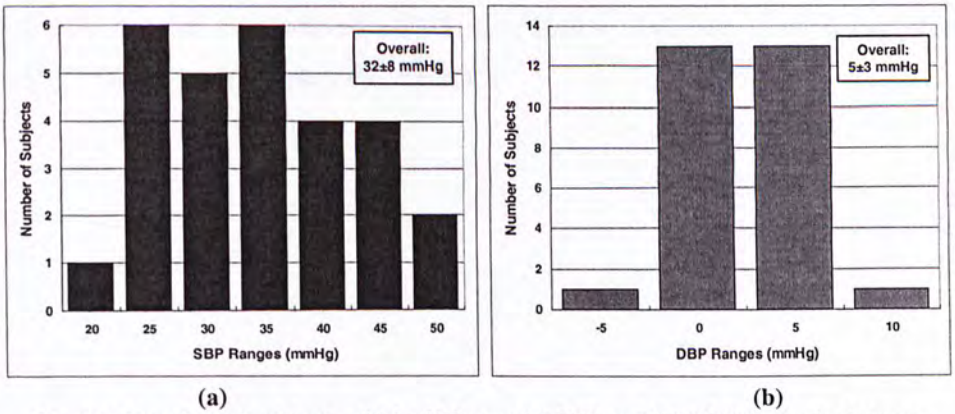

(a) (b)

Fig. 5.6: Number of subjects within different (a) SBP and (b) DBP dynamic changes.

5.1.4 Experimental Results

Effects of Hydrostatic Pressure on PTT and BP

Fig. 5.7 shows the effects of hydrostatic pressure on MBP and SBP from both resting arm and elevated arm with reference to MBP and SBP measured at H=0 cm for all 28 subjects . From Fig. 5.7 (a) and (c) it is noticed that there are little variations in brachial pressure (i.e. P_I in equation (4.8) and (4.9)) measured at the resting arm

during the arm elevation process. Yet it seems that there is no trend between these variations and the heights of subjects' elevated arms. These variations of brachial pressure measured from the resting arm are later corrected when calculating the changes of radial pressures measured from the elevated arm.

One of the assumptions of calibration equation (4.8) and (4.9) is that the arterial pressure changes equal to the hydrostatic pressure changes ($P_H=\rho gh$) caused by arm elevation. In order to verify this, the radial SBP as well as MBP at the elevated arm are measured and their changes with respected to those measured at H=0 cm are presented in Fig. 5.7 (b) and (d). Overall results show that the mean changes of radial MBP and SBP measured from elevated arm agree well with the theoretically calculated hydrostatic pressure ($P_H=\rho gH$).

The effects of hydrostatic pressure on PTT are presented in Fig. 5. 8 in which H=0 cm is selected as reference height level. Paired t-test is done for 24 out of 28 subjects whose PTT readings at 5 Hs are all available. In generally, the higher the arm is elevated, the longer the PTT observed from the elevated fingertip will be. It is shown that PTT at H=-20 cm and H=20 cm are significantly different from PTT at H=0 cm ($p<<0.01$). Moreover larger variations in PTT for positive heights than for negative heights can be observed (ΔPTT from H=0 to H=20 cm is significantly larger than ΔPTT from H=-20 to H=0 cm, $p<0.01$).

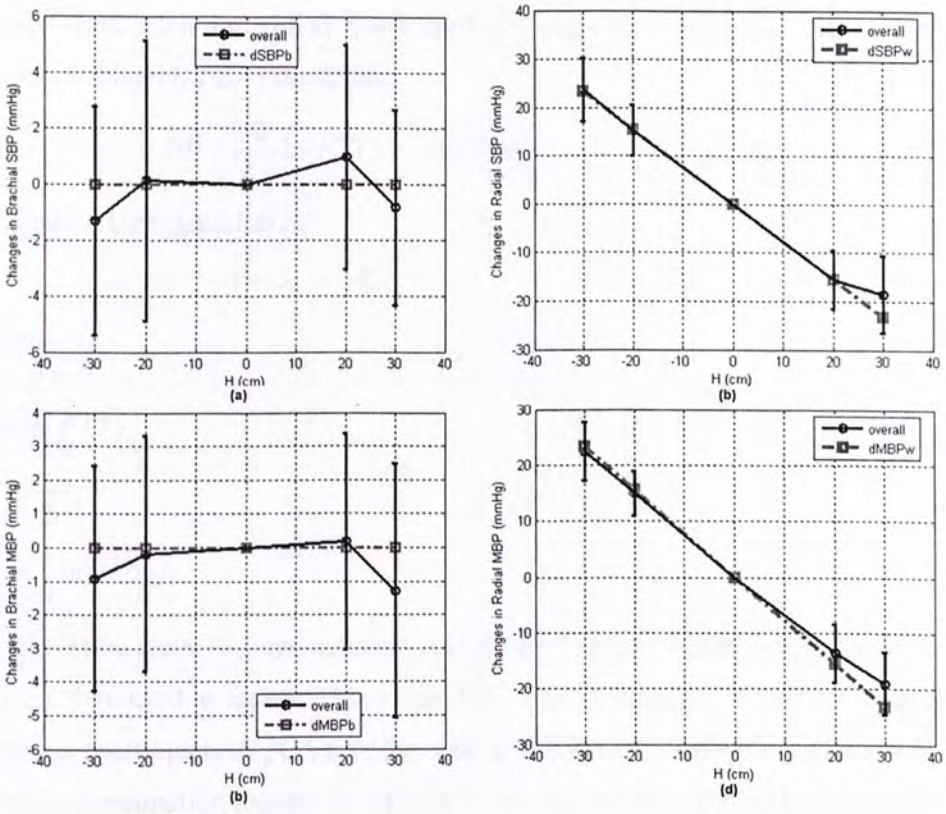

Fig. 5.7: Changes of (a) Brachial SBP, (b) radial SBP*, (c) Brachial MBP and (d) radial MBP* during the arm elevation process with respect to those measured at H=0 cm.

*** The vertical height of heart wrt. Shoulder is assumed as -10 cm**

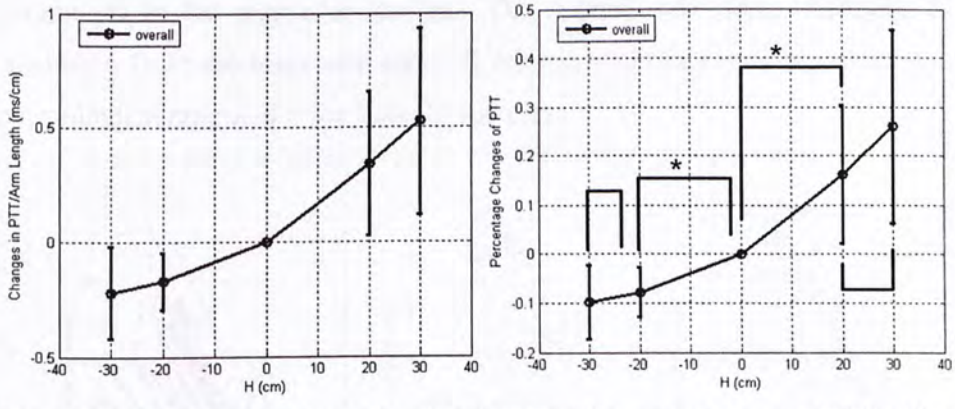

Fig. 5.8: (a) Changes of PTT over Arm length and (b) Percentage changes of PTT with respected those measured at H=0 cm.

*** denotes significant changes of PTT (p<<0.01).**

Optimal Results – Results from Regression Analysis

For each subject, the 1st trial of resting session (PTT_{r1}) is removed and all the other 5

datasets from each individual were used for regression analysis. Recalling the PTT-based model for BP estimation

$$BP = \frac{-2}{b} \cdot \ln(PTT) + \frac{1}{b} \ln(L^2 \rho b) \qquad \cdots (4.9),$$

the equation for regression is:

$$y = S_r \cdot x + C_r \qquad \cdots (5.1)$$

where:

$y = BP$;

$x = \ln(PTT)$;

$S_r = \frac{-2}{b}$;

$C_r = \frac{1}{b} \ln(L^2 \rho b)$;

The regression slope (S_r) and constant (C_r) for each subject together with the recorded PTTs are then used to estimate his or her BPs. The estimation results by using these regression coefficients (S_r, C_r) give the optimal prediction results for equation 4.9.

The overall estimation results for SBP and DBP are 0.00±2.67 mmHg and 0.00±1.44 mmHg, respectively. The overall estimation results for MBP and PP are even smaller: 0.00±1.46 mmHg and 0.00±1.43 mmHg, respectively. Fig. 5.9 shows the individual regression lines for each subject. Table 5.2 gives general descriptions of parameters in the regression results. The optimal individual coefficient b values calculated from the regression slope S_r are presented in Fig. 5.10, which shows the physiological ranges of b for these 28 subjects.

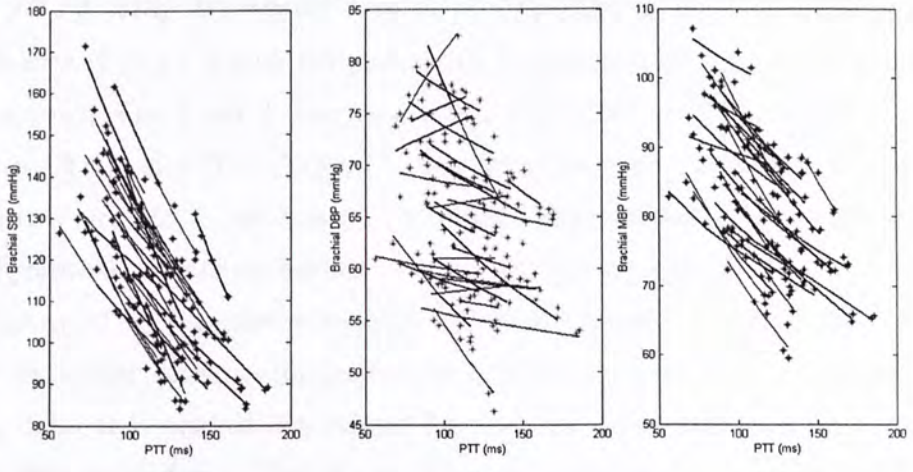

(a) (b) (c)

Fig. 5.9: Parameters measured (plotted as *) and regression lines for (a) PTT vs SBP, (b) PTT vs DBP and (c) PTT vs MBP.

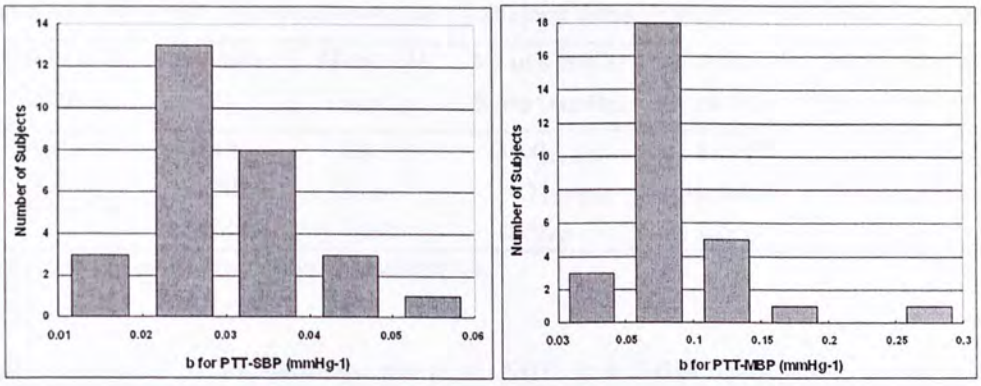

(a) (b)

Fig. 5.10: Number of subjects within different ranges of b for (a) PTT-SBP and (b) PTT-MBP.

Table 5.2: Individual correlation coefficient (r), b, S_r, C_r calculated in regression analysis and SD of BP estimation error by

	For PTT-SBP relationship	For PTT-MBP relationship
r (for *ln(PTT)* and *BP*)	-1.00 ~ -0.80 (-0.97±0.04)	-1.00~ -0.66 (-0.93±0.09)
b (mmHg-1)	0.01 ~ 0.06 (0.03±0.01)	0.03 ~ 0.28 (0.09±0.05)
S_r (mmHg)	-144 ~ -34 (-72±34)	-59 ~ -7 (-28±11)
C_r (mmHg)	-153 ~ 40 (-39±46)	-27 ~ 73 (21±26)
SD (mmHg)	0.6 ~ 6.0 (2.7±1.4)	0.3 ~ 3.0 (1.4±0.8)

Results by using Hydrostatic Calibration methods:

As described in 5.1.2, both two hydrostatic calibration methods, named hydrostatic calibration method I and II, take use 2 sets of PTTs (PTT1 and PTT2) and only differ at the selection of PTT1. Table 5.3 summarizes the overall estimation results using these two methods for all subjects participated in experiment I and II. It is found that hydrostatic calibration method II, which selects the 1st set of PTTs during resting session as PTT1, provides better MBP and SBP estimation results. Thus only the MBP estimation results using hydrostatic calibration method II is also presented in Table 5.3. It is marked that subject 2.6 tilted his upper parts of body during the calibration procedure. The results after removing datasets of subject 2.6 are presented in Table 5.3.

Table 5.3: Overall Estimation Results for All Subjects Using Hydrostatic Calibration Methods

Calibration Method	Estimated BP	Mean±SD (mmHg)	Mean Absolute Error (mmHg)	Mean±SD* (mmHg)	Mean Absolute Error* (mmHg)
Method I	SBP	8.6±9.3	$10.4\|_{H=20\ cm}$	8.4±9.5	$10.4\|_{H=20\ cm}$
Method II	SBP	-2.2±8.3	$6.3\|_{H=20\ cm}$	-2.8±7.7	$6.0\|_{H=20\ cm}$
	MBP	3.6±8.0	$5.5\|_{H=0\ cm}$	2.8±7.0	$4.8\|_{H=0\ cm}$

*** denotes the results after removing subject 2.6.**

Individual and Bland-Altman plots of SBP and MBP estimation errors using hydrostatic calibration method II are shown in Fig. 5.11 and Fig. 5.12, respectively. It is noticed in Fig. 5.12 that for MBP the estimation errors are larger when the estimated pressures are higher, while this is not the case for SBP.

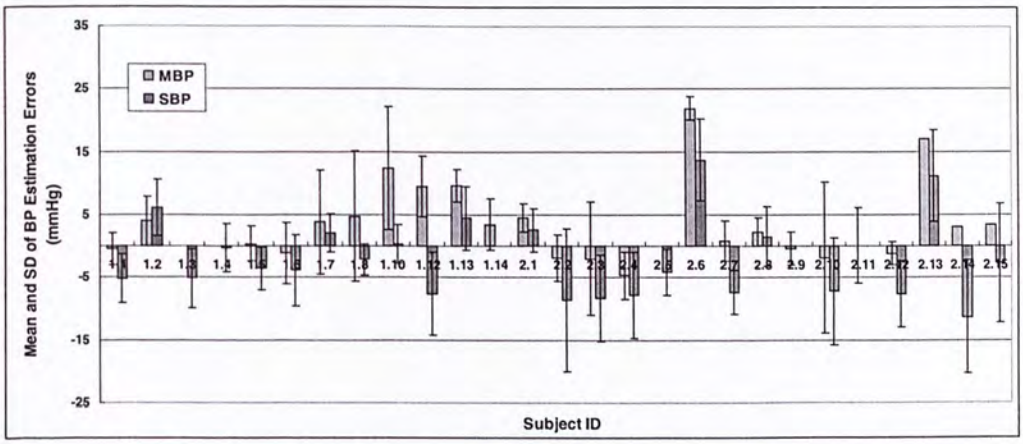

Fig.5.11 Individual estimation results for SBP and MBP using hydrostatic calibration method II.

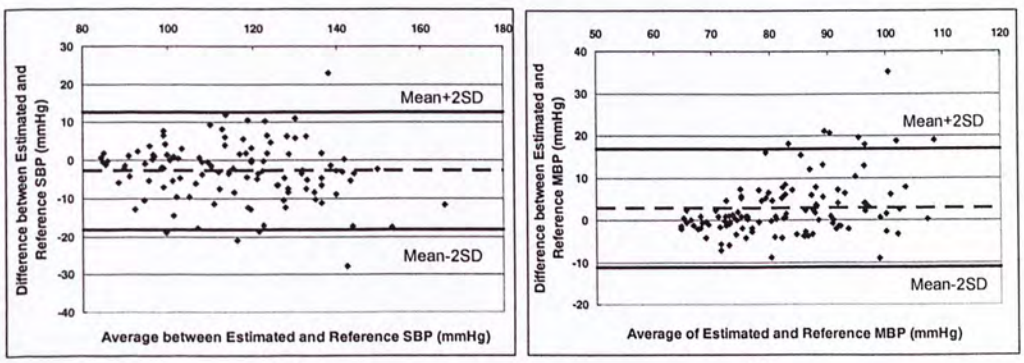

(a) **(b)**

Fig.5.12: Bland-Altman plot of (a) SBP and (b) MBP estimation errors using hydrostatic calibration method II.

Results by Other Method Using One Reference BP

Table 5.4 shows the prediction results for which no calibration is done, i.e. for each subject, his/her BP is always regarded as the BP obtained at the first time during resting status (BP_{r1}) as shown in equation (5.2).

$$BP \equiv BP_{ri} \tag{5.2}$$

Table 5.4: Predictions Results by Using One Reference BP (BP_{r1})

	$BP \equiv BP_{R1}$
SBP (mmHg)	-12.4 ± 13.5
DBP (mmHg)	-0.6 ± 3.6
MBP (mmHg)	-4.5 ± 5.8

5.2 Section Discussions

In this chapter, two experiments are carried out to verify the proposed hydrostatic calibration method and its implementation algorithms.

Two assumptions for the hydrostatic calibration method are: (1) heart pressure remains stable during calibration procedure and (2) the changes in peripheral arterial pressure can be approximated as hydrostatic pressure changes ($P_h=\rho \cdot g \cdot h$) are tested with the experimental data. In Fig. 5.7 (a) it is noticed that for all subjects the mean changes in brachial SBP and MBP remain stable during the whole arm elevation process. In Fig. 5.7 (b) it is observed that the mean changes in radial MBP are slightly smaller than P_H (i.e. changes in P_h with H), while the mean changes in radial SBP agree well with P_H except for H=30 cm at which the mean change in radial SBP is smaller than P_H by around 5 mmHg. The less changes of radial BP compared with theoretical values when the arm is elevated have been noticed and discussed in chapter 3. Overall, these two assumptions for the proposed calibration method are verified by the experimental results.

Noticed that in experiments discussed in this chapter there is an approximation, i.e. the vertical distance between heart and shoulder (P_{sh-h}) is regarded as 10 cm for all the subjects. This is because the major arteries (from ascending aorta to brachial arteries) are bent around shoulder due to the geographic changes of human body. The effects of curved arteries on PTT or BP have not been investigated and it may not be appropriate to apply the hydrostatic calibration equation on the whole arterial tree from heart to fingertip. Therefore, the level of shoulder is regarded as H=0 cm in this study and the BP at H=0 cm is approximated as BP at heart level minus the hydrostatic pressure change cause by the vertical distance between heart level and shoulder level. Overall, the measured BP differences between heart level and shoulder level are 5.8±4.7 mmHg for SBP and 4.6±3.5 mmHg for MBP, while the corresponding theoretical hydrostatic pressure is 7.8 mmHg ($\Delta P_h=\rho g H_{sh-h}$). The ΔP_h caused by H_{sh-h} need to be further investigated and repeated on more subjects. In this study however, the approximation is used since it greatly simplifies the calibration procedure and the estimation results are within reasonable ranges.

In chapter 3 the changes of PTT under the effects of hydrostatic pressure P_H for positive heights have been tested. In this experiment the effects of P_H on PTT for

both negative and positive heights are examined. Generally, PTT increases with H when heart pressure remains stable. Moreover, the results of this study further confirmed the unsymmetrical changes of PTT for H<0 and H>0, i.e. changes of PTT for positive Hs are larger than for negative Hs. The changes of PTT from PTT measured at H=0 cm (PTT_0) divided by PTT_0 (i.e., percentage change of PTT) are shown in Fig. 5.13. It can be observed that its increasing trend with H is consistent with the theoretical ΔPTT-H curve simulated according to equation (4.9).

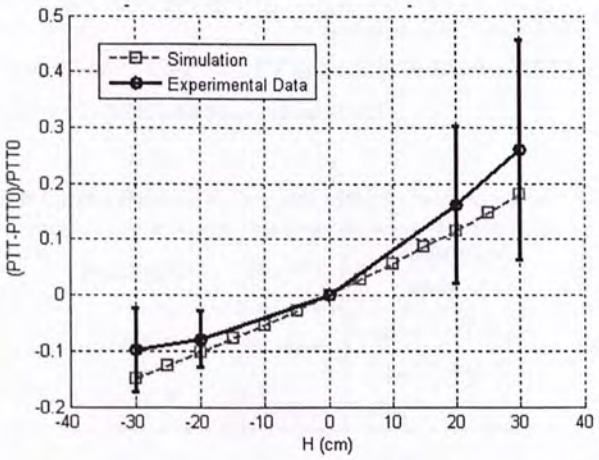

Fig. 5.13: Percentage change of PTT $(PTT_i\text{-}PTT_0)/PTT_0$ at different Hs plotted based on experimental data (solid line) and simulated results with b=0.03 $mmHg^{-1}$ (dashed line).

According to the mean absolute error (MAE) of individual SBP estimation results, five subjects with the worst MAE are separated from others and the percentage changes of PTT for these two groups are plotted in Fig. 5.14. The averaged value of $(PTT\text{-}PTT_0)/PTT_0$ for the worst 5 subjects are much higher than for other subjects as presented in Fig. 5.14 (a). Calculating the percentage change of PTT does not involve any cuff-based BP measurement and thus it is used in this study to test the validity of calibration. A threshold for $(PTT\text{-}PTT_0)/PTT_0$ is made tentatively and those not within the range of simulated $(PTT\text{-}PTT_0)/PTT_0 \pm 0.09$ are regarded as invalid calibration trials. The SBP estimation results after removing those subjects with invalid calibrations are presented shown in Table 5.5. It is found that both mean and SD of prediction errors are reduced for the hydrostatic calibration method. Besides, when compared with the traditional calibration method with an optimal slope for data collected in this experiment, the SBP prediction by using hydrostatic calibration method is significantly smaller in mean bias ($p<0.05$).

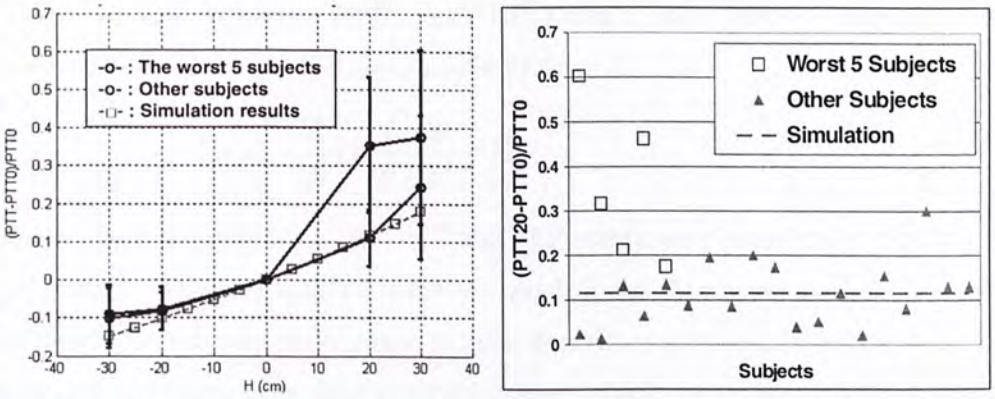

Fig. 5.14: (a) Mean and SD of (PTT-PTT$_0$)/PTT$_0$ and (b) individual (PTT-PTT$_0$)/PTT$_0$ from the worst 5 subjects, the other subjects and simulation results.

Table 5.5: SBP Estimation Results before and after Removing Invalid Calibration Trials

	Calibration Method	Mean±SD	MAE	Calibration Method	Mean±SD	MAE
Before	Hydrostatic Calibration	2.2±8.3	$6.3\|_{H=20\,cm}$	BP = k·PTT+C (k=-70 mmHg C=BP$_0$-k·PTT$_0$)	0.6±7.1	5.3
After		-0.6±7.4	$5.6\|_{H=20\,cm}$		1.9±7.5	5.6

Unit: mmHg

According to the determined threshold eight subjects are removed due to the invalidity of their calibration trials. The variation of (PTT-PTT$_0$)/PTT$_0$ could be measurement error or intrinsic change of PTT which may be introduced during PTT measuring session due to several factors: firstly, motion artifacts induced when subjects' arms are holding freely in the air; secondly, the transformation of PPG morphology when P_{tr} is reduced because of the increase of finger height; thirdly, the autoregulation mechanism in skeletal muscle. The percentage changes of PTT from three subjects who attended both experiment week I and II are compared for two different days. The results show that no subject has invalid calibration trials for both two days, and for two subjects their calibration trials are invalid for one day and valid for the other day. This preliminary result indicates that the invalidity of calibration trial is possibly contributed by measurement error. However, the repeatability and feasibility of utilizing percentage change of PTT for validity test need to be further verified.

An important implementation of the proposed hydrostatic calibration method is that in this study, PTT is used for SBP estimation, while equation (4.3) and/or (4.4) describes

the relationship between PTT' (*PTT'=PTT-PEP*) and MBP. Therefore, the theoretical curves simulated from equation (4.3)

$$BP = P_1 = \frac{1}{b}\ln(\frac{L^2 \rho b}{PTT^2} - 1) \tag{4.3}$$

and the experimentally measured PTT and SBP values are plotted in Fig. 5.15 (a) for comparison. The arm length *L* used for simulation is 70 cm, which is the averaged arm length for subjects participated in these experiments (shown in Table 5.1). The range of b is chosen from 0.02 to 0.08 $mmHg^{-1}$, which is the observed physiological range of b for the involved subjects as shown in Fig. 5.10. Individual PTT-SBP data measured in the experiments are plotted with different colors and markers. A regression line for the experimental PTT-SBP data calculated using the 2^{nd} order polynomial regression is drawn, and it could be visually found that this regression line follows the trend of theoretical PTT'-MBP curves.

However, it is noticed that the experimental data locate at the upper and right side of the theoretically simulated PTT'-MBP curves. In the calibration session, b is calculated from 2 PTT readings using equation (4.9) and thus the curvature of PTT-SBP curve is determined. In the estimation session, the calibrated b and PTT are substituted into equation (4.4) in which PTT' should be used to predict MBP. Therefore, the 'SBP' values calculated in this way cluster at the areas restricted by theoretical PTT'-MBP curves, and are somewhat smaller than real SBP values since MBP is known to be lower than SBP for a particular subject. This contributes to the bias between estimated SBP and reference SBP and in this study, this bias is individually corrected by using the reference SBP corresponding to PTT_1.

Fig. 5.15 (b) gives a set of simulated PTT'-MBP curves with different L and b values. For a given range of PTT' values, the PTT'-MBP curve can be determined by two individual parameters: L and b. The experimental PTT-MBP and PTT-SBP data together with the simulated PTT'-MBP curves are plotted in Fig. 5.15 (c). As mentioned above, the scatter plots of PTT-SBP data mainly locate at the upper and right side of the area that is restricted by theoretically simulated curves. On the other hand, the scatter plots of PTT-MBP data look like somewhat right shifted. This could be understood since *PTT'=PTT-PEP*. It can be observed that the scatter plots of compressed PTT (e.g. (75% PTT) and MBP are almost overlapped with the area restricted by theoretically simulated PTT'-MBP curves (Fig. 5.16).

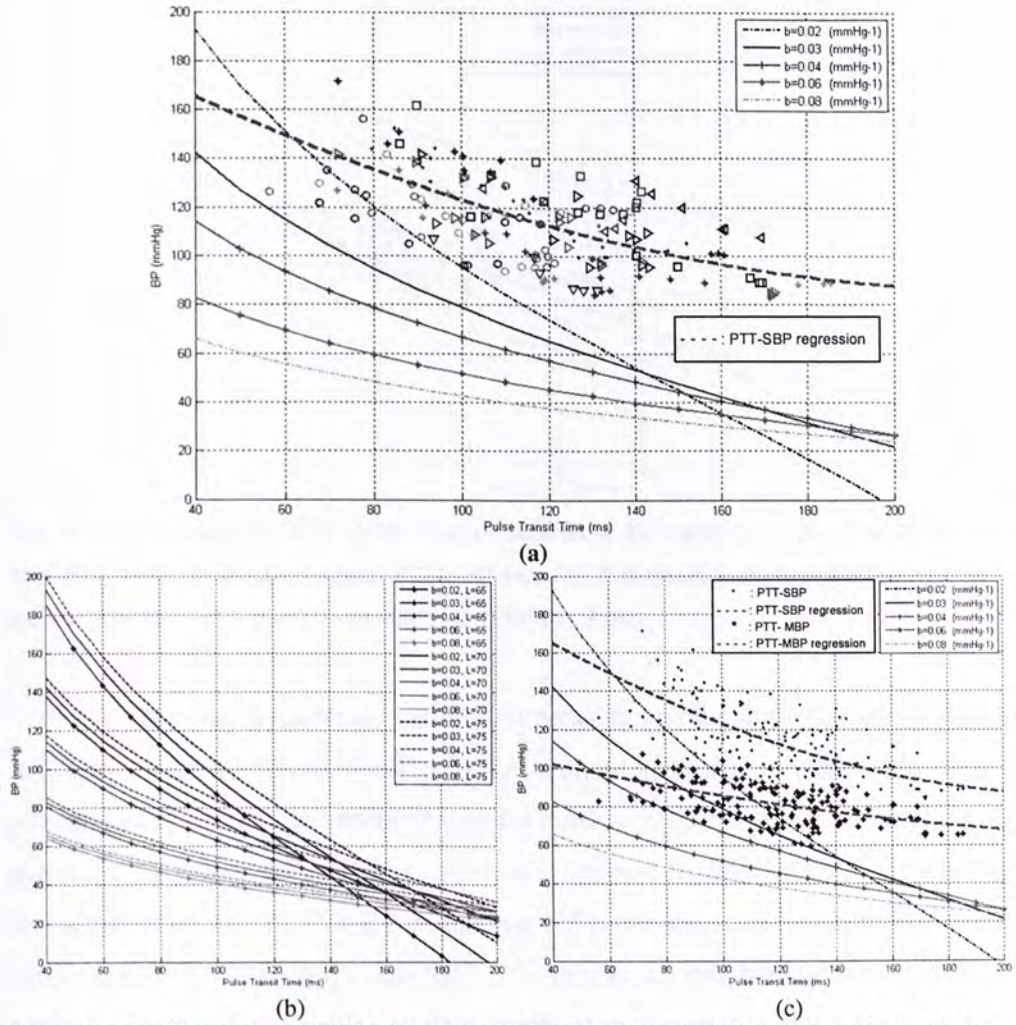

Fig. 5.15: (a) Theoretical PTT'-MBP curves simulated by equation (4.3) with L=70 cm, and experimental PTT-SBP data from 28 subjects in scatter plot (Regression curve for all PTT-SBP data: $y = 0.0022*x^2-1.0151*x+202.68$), (b) Simulated PTT'-MBP curves with different L and b values. Units for (c): L (cm) and b ($mmHg^{-1}$), and (c) Theoretical PTT'-MBP curves simulated by equation (4.3) with L=70 cm, and experimental PTT-MBP data from 28 subjects in scatter plot (Regression curve for all PTT-MBP data: $y = 0.0006*x^2-0.3585*x+115.56$).

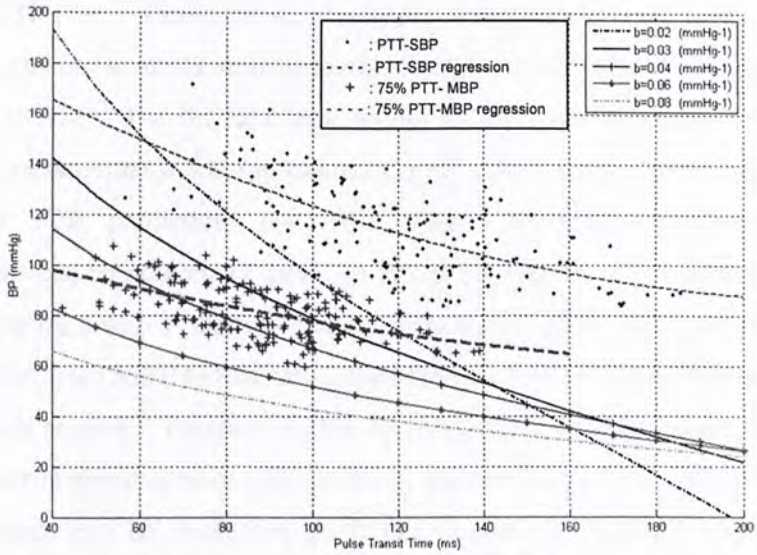

Fig. 5. 16: Theoretical PTT'-MBP curves simulated by equation (4.3) with L=70 cm, and 75%PTT-MBP from experimental PTT-SBP data for 28 subjects in scatter plot (Regression curve for all 75%PTT-MBP data: $y = 0.001*x^2-0.4779*x+115.56$).

With the proposed hydrostatic calibration pressure and the implementation algorithm, it is now able to calibrate b cufflessly, i.e. without using any reference BP. Fig. 5.16 schematically shows the potential way for cuffless calibration and estimation of MBP using 2 PTT values only (PEP is assumed to account for 25% of PTT). Nevertheless, the application of PTT'-MBP model on PTT introduced a pressure bias between estimated BP and the reference SBP. In this study, this bias is corrected by using SBP_1 which is corresponding to PTT_1 while at the mean time this correction induced an initial use of cuff-based BP reading.

A complete cuffless calibration and MBP estimation method using PTT' measured from wrist to the base of index finger is reported in a very updated research work by McCombie *et.al* [109]. Their model is developed based on the concept of integrating lumped PWV model along a specific length as we first raised in chapter 3. The calibration method utilizes both hydrostatic and external pressure changes during arm and hand movements to calculate all the model coefficients. Though the assumptions of their model suffer challenges and the available prediction data are very limited and only for resting condition, their method has received complete cuffless MBP estimation results at the same order of reference MBP. Comparing with their approach, our method aimed at utilizing PTT for cuffless calibration and SBP measurement since SBP is clinically used and PTT is reported to be more highly

related to SBP [39]. Based on what we have achieved there are mainly two steps needed towards our goal: the transformation from PTT to PTT' and the transformation from MBP to SBP. For the first step, research work have been done to investigate convenient measurements for approximated PEP values [110, 111] or computational models for PEP prediction using PTT based on their correlation. These investigations can be potentially used combining the presented hydrostatic calibration method to realize cuffless calibration and estimation for MBP. For the second step, a transformation from MBP to SBP with parameters that do not contain arterial pressure information is needed. Previous studies have demonstrated that waveforms between PPG and arterial pressure have high similarity and the normalized PPG waveform can be transformed into BP waveform cufflessly [112-114]. Thus it may be able to calculate the MBP-SBP ratio based on PPG morphology so that the initial use of cuff-based BP can be avoided.

As discussed in chapter 4, the BP-PTT and $BP_{peripheral}$-PTT curves determined by the same b for a specific subject differ in curvatures. Therefore, algorithms that regarding these two as linear curves, and applying the feature coefficients (such as slope and intercept) calibrated from $BP_{peripheral}$-PTT curve to the BP-PTT model for BP prediction may not be that appropriate. Fig. 5.17 plotted the PTT, brachial SBP and radial SBP data recorded in experiment week I and II from three subjects whose b values vary from around 0.01 to 0.06 $mmHg^{-1}$. Since the arm length for the three subjects are different, their PTT and pressure data are plotted separately. It can be observed that the experimental results show similar pattern with the theoretically simulated curves for different b values.

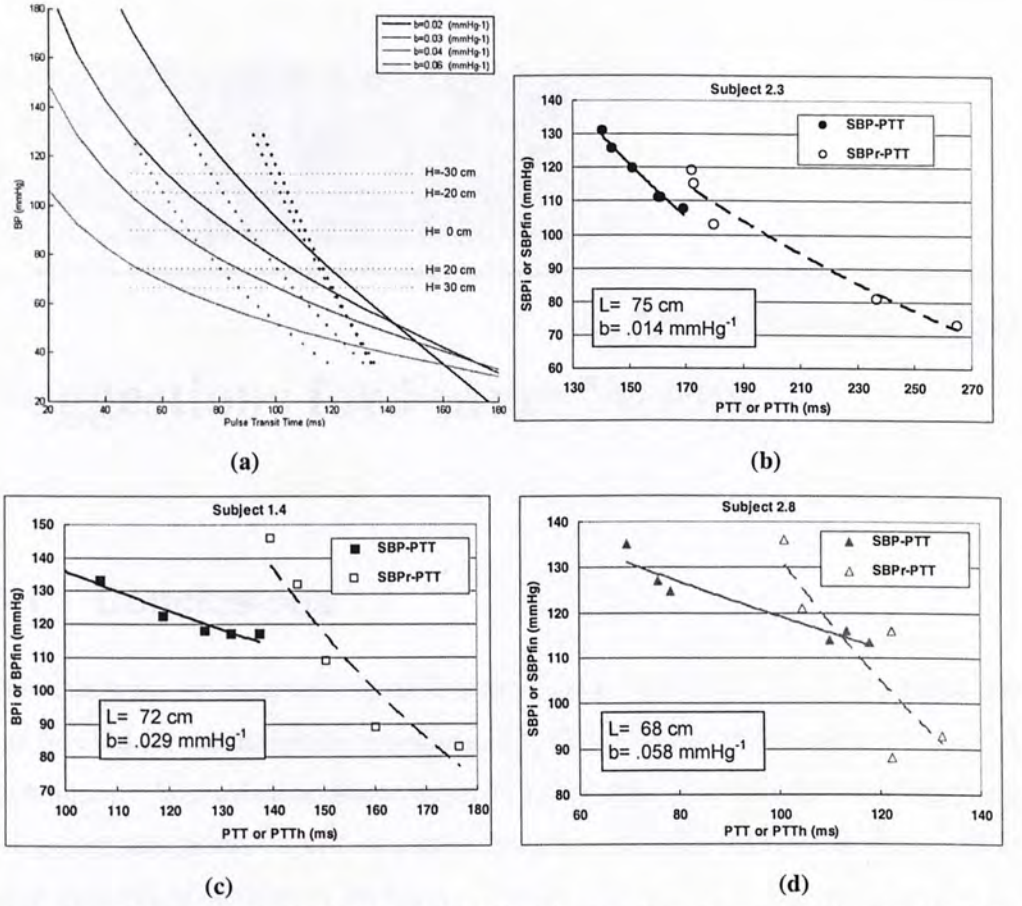

Fig. 5. 17: (a) Simulated MBP-PTT' and MBP_f-PTT' curves from equation (4.9) given L=70 cm and b={.02, .03, .04, .06} $mmHg^{-1}$, as well as typical SBP-PTT and SBPr-PTT data from subjects with different b: (b) subject 2.3, (c) subject 1.4 and (c) subject 2.8. .

5.3 Section Summary

In this chapter the experimental results for testing the proposed model-based hydrostatic calibration approach and its implementations are presented. The results obtained from the theoretical analysis of the model are compared against data acquired from the experimental studies. Two assumptions of the model are verified and two approximations made for the implementation are discussed. Based on the experimental results of this study, the proposed calibration approach can be used to calibrate individual coefficients and the overall estimation results using this approach are within the required standard. Furthermore, based on this calibration model, it is possible to further develop a completely cuffless calibration approach. The PTT-based hydrostatic calibration method proposed in this study involves simple movements and can be used for the design of wearable BP devices.

CHAPTER 6

Conclusions and Suggestions for Future Works

6.1 Conclusions

This thesis has been carried out to investigate a model-based calibration method that can be used for the design of wearable and cuffless BP devices that are based on PTT techniques. Towards this objective, studies have been done mainly focusing on the following three parts. The first part of this thesis identified the factors that could be used to develop calibration methods. Factors with the following two features are preferred: 1) they can induce BP and/or PTT changes from which the characteristic coefficients of a PTT-BP model can be obtained and 2) the involved procedures are easy to be implemented and the required equipment can be integrated to wearable devices for BP measurements. Finally the external cuff pressure (P_E) and hydrostatic pressure (P_H) are selected among various factors and their effects on PTT and BP are investigated.

The second part of this thesis focused on the theoretical study of pulse transmission through arteries. A model is built up through studying the effects of P_H on PTT during arm elevation, and a bio-model based hydrostatic calibration approach is further developed. Besides, a new implementation algorithm for this hydrostatic calibration model is proposed. Through this model the individual coefficient can be obtained cufflessly. Theoretical simulations are conducted based on the proposed calibration and estimation models.

The third part of this thesis is focused on experimental studies to test the proposed hydrostatic calibration approach. The experiment which involves 28 subjects includes an arm-elevation process for calibration and a dynamic exercise process that

could induce large BP variations. The experimental data are compared with the simulation results. It is found that experimental results for testing the two important assumptions of the calibration model: 1) heart pressure remains stable during the calibration process, and 2) the changes of peripheral arterial BP equals to ΔP_H agree well with the theoretical simulation results. Besides, the experimental data describing percentage changes of PTT under the effects of P_H during arm elevation process as well as individual P_H-PTT and BP-PTT curves also follow the pattern of theoretical simulations. Furthermore, the percentage change of PTT is used for testing the validity of calibration trials. When the proposed calibration model is used for BP estimation, the results show that it can provide arterial BP with an overall estimation error within the AAMI standard; and when those subjects with invalid calibration are removed, both mean and SD of the estimation results are significantly reduced.

In summary, this thesis deals with a systematic study on the development of a bio-model based calibration approach to meet the needs of wearable and cuffless BP devices. The proposed calibration method involves simple arm movements and calibrates the individual model coefficient using only two PTT values. This calibration approach is utilized by a BP estimation model based on PTT technique to estimate SBP before and immediately after dynamic exercise, and it gives a result within the AAMI standard. Moreover, the proposed calibration approach has the potential to be further developed to realize a complete cuffless BP calibration and estimation process.

6.2 Suggestions for Future Works

Further Modification of the Proposed Model for Hydrostatic Calibration

The model-based hydrostatic calibration approach proposed in this study has an advantage of obtaining the individual coefficient cufflessly, however it is found that during the estimation process, there exists a pressure bias between the predicted and the reference BP values. This bias is mainly generated during the process in which the theoretical BP-PTT' model is used to describe SBP-PTT relationship. To eliminate this bias, it is suggested to further study the relationship between mean arterial BP and systolic BP as well as relationship between different components of PTT. With these two aspects examined it is then possible to build up a model that

can directly relate PTT to systolic BP and thus lead to a complete cuffless BP calibration and estimation.

Further Verification of the Proposed Model for Hydrostatic Calibration

In this thesis the basic BP-PTT model is applied for segmental artery and further integrated for the whole arterial tree to develop the model for hydrostatic calibration method. It is noticed that the radius of arteries from main arteries (e.g. brachial artery at upper arm) to peripheral arteries (e.g. digital arteries at fingers) reduces and the bifurcations from radial artery to digital arteries do not strictly follow the cylindrical artery model in the model assumption. A preliminary study has been done (not presented in this thesis) in which three PPG sensors are located at elbow, wrist and index fingertip respectively to measure the segmental PWV values. Yet it is found that the recording force of PPG sensors at upper stream of arteries would cause changes in PWV readings obtained from down stream arteries. Besides, PTT values from radial wrist to fingertip are very small and are with the same order of measurement errors. Therefore it may need ultrasound or other imaging techniques to examine the effects of geographic changes of arteries on PTT changes to further verify the hydrostatic model.

Further Verification of the Proposed Calibration Approach on Larger Subject Pool

In this thesis the proposed hydrostatic calibration approach has been tested for subjects aged from around 20 to 40 years old with a dynamic exercise process. It is known that subjects with cardiovascular diseases like hypertension would have changes in the elastic properties of arterial wall and thus undergo larger variations of BP. The proposed calibration approach which involves only simple arm movements is thus suitable for most subjects and is suggested to be tested for elderly subjects or subjects with reported cardiovascular diseases for more wide applications.

Reduction of Motion Artifacts

It is known that motion artifacts will induce noises into the ECG and PPG signals and contribute to estimation errors. The wearable BP devices aim at monitoring BP without disturbing daily activities and moreover, the calibration process involves arm elevation processes. Thus it is necessary to further improve the configurations and designs of ECG and PPG sensors to eliminate the noises induced by motion artifact.

Reference

1. T. Thom, et al., *Heart Disease and Stroke Statistics--2006 Update: A Report From the American Heart Association Statistics Committee and Stroke Statistics Subcommittee*. 2006. p. e85-151.
2. P. M. Kearney, et al., *Global burden of hypertension: analysis of worldwide data.* The Lancet, 2005. **365**(9455): p. 217-223.
3. L. E. Fields, et al., *The Burden of Adult Hypertension in the United States 1999 to 2000: A Rising Tide*. 2004. p. 398-404.
4. K. Wolf-Maier, et al., *Hypertension Treatment and Control in Five European Countries, Canada, and the United States*. 2004. p. 10-17.
5. R. R. Joffres, et al., *Distribution of blood pressure and hypertension in Canada and the United States.* Am J Hypertens, 2001. **14**(11): p. 1099-1105.
6. S. S. Franklin, *Systolic blood pressure: It's time to take control.* American Journal of Hypertension, 2004. **17**(12, Supplement 1): p. S49-S54.
7. K. Wolf-Maier, et al., *Hypertension Prevalence and Blood Pressure Levels in 6 European Countries, Canada, and the United States*. 2003. p. 2363-2369.
8. C. C. Y. Poon, *A Bio-model-based Cuffless Technique for Non-invasive and Continuous Measurement of Arterial Blood Pressure*, in *Dept. of Electronic Engineering*. 2006, The Chinese University of Hong Kong: Hong Kong.
9. G. Bakris, et al., *Achieving blood pressure goals globally: five core actions for health-care professionals. A worldwide call to action.* J Hum Hypertens, 2007. **22**(1): p. 63-70.
10. J. G. Webster and J.W. Clark, *Medical Instrumentation: Application and Design*. 3rd ed. 1998, New York: Wiley.
11. S. W. Cohen. *Effects of age on blood pressure* 2006 [cited; Available from: http://www.nlm.nih.gov/medlineplus/ency/imagepages/8693.htm.
12. C. C. Y. Poon and Y. T. Zhang. *Using the Changes in Hydrostatic Pressure and Pulse Transit Time to Measure Arterial Blood Pressure*. in *Proc. 29th Annu. Int. Conf. of IEEE Engineering in Medicine and Biology Society*. 2007. Lyon, France.
13. T. Chen. *Wrist Blood Pressure Monitor (Model No: LF-01).* [cited 2008; Available from: http://www.living-forever.com/bp-e.htm.
14. J. Peňáz, *Photo-electric measurement of blood pressure, volume and flow in the finger.* Digest of the 10th Int. Conf. on Medical and Biolog. Eng., 1973: p. 104.
15. N. T. Smith, K. H. Wesseling, and B. de Wit, *Evaluation of two prototype devices producing non-invasive, pulsatile, calibrated blood pressure measurement form a finger.* J. Clin. Monit., 1985. **1**: p. 17-29.
16. K. H. Wesseling, et al., *Physiocal, calibrating finger vascular physiology for Finapres.* Homeostasis, 1995. **36**: p. 67-82.
17. G. L. Pressman and P.M. Newgard, *A Transducer for the Continuous External Measurement of Arterial Blood Pressure*. Bio-Medical Electronics, IRE Transactions on, 1963. **10**(2): p. 73-81.
18. M. D. Driscoll, J. M. Arnold, and M.H. Sherebrin., *Applied recording force and noninvasive arterial pulses.* Clin Invest Med., 1995. **18**(5): p. 370-379.
19. M. D. Driscoll, et al., *Determination of appropriate recording force for non-invasive measurement of arterial pressure pulses.* Clinical Science, 1997. **92**(6): p. 559-566.

20. J. C. Bramwell and A.V. Hill. *The velocity of the pulse wave in man.* in *Proceedings of the Royal Society*. 1922. London.
21. J. C. Bramwell and A.V. Hill, *Velocity of transmission of the pulse wave and elasticity of arteries.* The Lancet, 1922(6): p. 891-892.
22. J. M. Steele, *Interpretation of arterial elasticity from measurements of pulse wave velocities.* The American Heart Journal, 1937. **14**: p. 452-465.
23. A. P. G. Hoeks, et al., *Non-invasive measurement of mechanical properties of arteries in health and disease.* Proc. Instn. Mech. Engrs., 1999. **213 Part H**: p. 195-202.
24. M. F. O'Rourke and G. Mancia, *Arterial stiffness.* Journal of Hypertension, 1999. **14**: p. 1-4.
25. G. L. Woolam, et al., *The pulse wave velocity as an early indicator of atherosclerosis in diabetic subjects.* Circulation, 1962. **25**: p. 533-539.
26. H. Smulyan, et al., *Forearm arterial distensibility in systolic hypertension.* J. Am Coll Cardiol, 1984. **3**: p. 387-393.
27. J. J. Toto-Moukouo, et al., *Pulse wave velocity in patients with obesity and hypertension.* Am Heart J., 1986. **112**: p. 112-136.
28. R. Ross, *Atherosclerosis an inflammatory disease.* New England Journal of Medicine, 1999. **340**: p. 115–126.
29. G. S. Malindzak and J.H. Meredith, *Comparative study of arterial transmission velocity.* J. Biomech., 1970. **3**: p. 337-350.
30. P. D. McCormack, *Doppler Monitoring of the Peripheral Vascular Status of Human Subject under Variable Arterial Pressure.* 1981. Naval Aerospace Medical Research Laboratory: Pensacola, FL.
31. M. W. Ramsey, *Real time measurement of pulse wave velocity from arterial pressure waveforms.* Med. Biol. Eng. Comput., 1995. **33**: p. 636-643.
32. I. B. Wikinson, *Pulse analysis and arterial stiffness.* J. Cardiovasc. Pharmacol., 1998. **32**: p. S33-37.
33. M. Persson, H. Eriksson, and K. Lindstrom. *Estimation of arterial pulse wave velocity with a new tissue Doppler method.* in *Proc.23rd Ann. Int. Conf. of IEEE Engineering in Medicine and Biology Society*. 2001. Istanbul.
34. A. Steptoe, H. Smulyan, and B. Gribbin, *Pulse Wave Velocity and Blood Pressure Change: Calibration and Applications.* Psychophysiology, 1976. **13**(5): p. 488 – 493.
35. P. A. Obrist, et al., *Pulse transit time: relationship to blood pressure and myocardial performance.* Psychophysiology, 1979. **16**(3): p. 293-301.
36. L. A. Geddes, et al., *Pulse Transit Time as an Indicator of Arterial Blood Pressure.* Psychophysiology, 1981. **18**(1): p. 71 – 74.
37. R. Allen, et al., *The Covariation of Blood Pressure and Pulse Transit Time in Hypertensive Patients.* Psychophysiology, 1981. **18**(3): p. 301 – 306.
38. G. V. Marie, et al., *The relationship between arterial blood pressure and pulse transit time during dynamic and static exercise.* Psychophysiology, 1984. **21**(5): p. 521-527.
39. R. A. Payne, et al., *Pulse transit time measured from the ECG: an unreliable marker of beat-to-beat blood pressure.* J. Appl Physiol, 2006. **100**: p. 136-141.
40. D. J. Hughes, et al., *Measurement of Young's modulus of elasticity of the canine aorta with ultrasound.* Ultrasonic Imaging, 1979. **1**: p. 356-367.
41. J. A. Posey and L. A. Geddes, *Measurement of the modulus of elasticity of the arterial wall.*

Cardiovasc. Res. Cent. Bull., 1973. **11**: p. 83-103.

42. M. F. O'Rourke, et al., *Pressure wave transmission along the human aorta.* Circ. Res., 1968. **23**: p. 567-579.
43. R. D. Latham, et al., *Regional wave travel and reflections along the human aorta: a study with sic simultaneous micromanometric pressures.* Circulation, 1985. **72**: p. 1557-1569.
44. Ramsey, M.W., W.R. Stewart, and C.J.H. Jones, *Real-time measurement of pulse wave velocity from arterial pressure waveforms.* Med. Biol. Eng. Comput., 1995. **33**: p. 636-642.
45. E. D. Lehmann, et al., *Validation and reproducibility of pressure-corrected aortic distensibility measurements using pulse wave velocity Doppler ultrasound,.* J. Biomed. Eng., 1993. **15**: p. 221-228.
46. M. Okada, S. Kimura, and M. Okada, *Estimation of arterial pulse wave velocities in the frequency domain: method and clinical considerations.* Med. Biol. Eng. Comput., 1986. **24**: p. 255-260.
47. S. Loukogeorgakis, et al., *Validation of a device to measure arterial pulse wave velocity by a photoplethysmographic method.* Physiological Measurement, 2002. **23**(3): p. 581-596.
48. A. B. Hertzman and C.R. Spielman, *Observations on the finger volume pulse recorded photoelectrically.* Am. J. Physiol., 1937. **119**: p. 334-335.
49. A. B. Hertzman, *The blood supply of various skin area as estimated by the photoelectric plethysmography.* Am. J. Physiol, 1938. **124**: p. 328-340.
50. J. Allen and A. Murray, *Similarity in bilateral photoplethysmographic peripheral pulse wave characteristics at the ears, thumbs and toes.* Physiological Measurement, 2000. **21**(3): p. 369-377.
51. E. A. López-Beltrán, et al., *Noninvasive studies of peripheral vascular compliance using a non-occluding photoplethysmographic method.* Med. Biol. Eng. Comput., 1998. **36**: p. 748-753.
52. K. Nakajima, T. Tamura, and H. Miike, *Monitoring of heart and respiratory rates by photoplethysmography using a digital filtering technique.* Medical Engineering & Physics, 1996. **18**(5): p. 365-372.
53. A. Johansson and P.Å. Öberg, *Estimation of respiratory volumes from the photoplethysmographic signal. Part I: experimental results.* Med. Biol. Eng. Comput., 1999. **37**: p. 42-47.
54. M. H. Pollak and P.A. Obrist, *Aortic-Radial Pulse Transit Time and ECG Q-Wave to Radial Pulse Wave Interval as Indices of Beat-By-Beat Blood Pressure Change.* Psychophysiology, 1983. **20**(1): p. 21 - 28.
55. J. D. Lane, et al., *Pulse Transit Time and Blood Pressure: An Intensive Analysis.* Psychophysiology, 1983. **20**(1): p. 45 - 49.
56. H. H. Hardy and R.E. Collins, *On the pressure-volume relationship in circulatory elements.* Med. Biol. Eng. Comput., 1982. **20**: p. 565-570.
57. F. K. Forster and D. Turney, *Oscillometric determination of diastolic, mean, and systolic blood pressure-a numerical model.* J. Biomech. Eng., 1986. **108**: p. 359-364.
58. Y. Tardy, et al., *Non-invasive estimate of the mechanical properties of peripheral arteries from ultrasonic and photoplethysmographic measurements.* Clin. Phys. Physiol. Meas., 1991. **12**(1): p. 39-54.
59. P. van Loon, W. Klip, and E.L. Bradley, *Length-force and volume-pressure relationship of*

arteries. Biorheology, 1977. **14**: p. 181-201.

60. K. Hayashi, et al., *Stiffness and elastic behavior of human intracranial and extracranial arteries.* J. Biomech., 1980. **13**(175-184).
61. G. J. Langewouters, K. H. Wesseling, and W. J. A. Goedhard, *The static elastic properties of 45 human thoracic and 20 abdominal aortas in vitro and the parameters of a new model.* J. Biomech., 1984. **17**: p. 425-435.
62. J. Megerman, et al., *Noninvasive measurements of nonlinear arterial elasticity.* Am. J. Physiol., 1986. **250**: p. H181-H188.
63. T. Kawasaki, et al., *Non-invasive assessment of the age related changes in stiffness of major braches of the human arteries.* Cardiov. Res., 1987. **21**: p. 678-687.
64. T. Powalowski and B. Pensko, *A noninvasive ultrasonic method for the elasticity evaluation of the carotid arteries and its application in the diagnosis of the cerebrovascular system.* Arch. Acoustics, 1988. **13**: p. 109-126.
65. P. Gizdulich and K. H. Wesseling, *Forearm arterial pressure-volume relationships in man.* Clin. Phys. Physiol. Meas., 1988. **9**: p. 123-132.
66. B. R. Simon, *Large deformation analysis of arterial cross-section.* Basic Eng., 1971. **93**: p. 138-146.
67. D. N. Ghista, G. Jayaraman, and H. Sandler, *Analysis for the noninvasive determination of arterial properties and for transcutaneous continuous monitoring of arterial blood pressure.* Med. Biol. Eng. Comput., 1978. **16**: p. 715-726.
68. A. L. King, *Pressure-volume relation for cylindrical tubes with elastometric wall: the human aorta.* J. Appl. Physiol., 1946. **17**: p. 501-505.
69. P. Niederer, *A molecular study of the mechanical properties of arterial vessel walls.* Z. Angew. Phys., 1974. **25**: p. 565-577.
70. P. Shaltis, A. Reisner, and H. Asada. *A hydrostatic pressure approach to cuffless blood pressure monitoring.* in *Engineering in Medicine and Biology Society, 2004. IEMBS '04. 26th Annual International Conference of the IEEE.* 2004.
71. D. B. Doublin and A. A. Rovick, *Influence of vascular smooth muscle on contractile mechanics and elasticity of arteries.* American Journal of Physiology, 1969. **217**: p. 1644–1651.
72. K. M. Van De Graaff, *Human Anatomy*. 5th ed. 1999, New York: McGraw-Hill.
73. W. W. Nichols and M. F. O'Rourke, *McDonald's blood flow in arteries : theoretical, experimental, and clinical principles* 5th ed. ed. 2005, New York: Oxford University Press.
74. W. W. Nichols and D. G. Edwards, *Arterial Elastance and Wave Reflection Augmentation of Systolic Blood Pressure: Deleterious Effects and Implications for Therapy*. 2001. p. 5-21.
75. H. Hosaka, et al., *Pulse-wave propagation time basis blood pressure monitor.* July 22, 1997: U.S. Patent 5,649,543.
76. H. Cecil, et al., *Continuous non-invasive blood pressure monitoring method and apparatus.* Jan. 25, 2003: C.A. Patent 2,353,807.
77. Y. Q. Chen, et al., *Continuous non-invasive blood pressure monitoring method and apparatus* Jul. 29, 2003: U. S. Patent 6,599,251.
78. Y. Q. Chen, et al., *Continuous non-invasive blood pressure monitoring method and apparatus.* May 17, 2005: U. S. Patent 6,893,401.
79. HOSAKA HIDEHIRO, N.T., *et al.*, *Multi-functional blood pressure monitor*, N.K. CORP.

Editor. 1997.

80. ONO KOHEI, K.H., *et al.*, *Blood pressure monitoring apparatus*, N.K. CORP, Editor. 1998: US.

81. M. S. Yu, S. L. LU, and C. Y. ZHANG, *Method for Measuring Arterial Blood Pressure by Using Pulse Wave and Apparatus Thereof*. Feb. 5, 1997: C. N. Patent 1,141,762

82. W. R. John, *Method of calibrating a blood pressure monitoring apparatus*. Apr. 21, 2004: G. B. Paten 2,394,178

83. A. K. Mills, *Device and method for noninvasive continuous determination of physiologic characteristics*. Mar. 25, 2003: U. S. Patent 6,537,225.

84. H. Inukai and H. Sakai, *System and method for evaluating the circulatory system of a living subject*. July 13, 1999: U. S. Patent 5,921,936.

85. Y. Sugo and T. Sohma, *Blood pressure measuring apparatus*. Jan. 20, 1998: U. S. Patent 5,709,212.

86. T. Ogura and H. Inukai, *Blood pressure monitor apparatus*. Feb. 8, 2000: U. S. Patent 6,022,320.

87. T. Ogura and H. Inukai, *Blood pressure monitor apparatus*. May 19, 1998: U. S. Patent 5,752,920.

88. Y. S. Yan and Y.T. Zhang. *A Novel Calibration Method for Noninvasive Blood Pressure Measurement Using Pulse Transit Time*. in *4th IEEE/EMBS International Summer School and Symposium on Medical Devices and Biosensors*. 2007.

89. Y. S. Yan and Y.T. Zhang. *A Model-based calibration method for noninvasive and cuffless measurement of arterial blood pressure*. in *IEEE Biomedical Circuits and Systems Conf. 2006*. 2006. London.

90. S. Aso, et al., *Blood pressure monitoring system*. Oct. 15, 1996: U. S. Patent 5,564,427.

91. C. C. Y. Poon and Y. T. Zhang. *Using the Changes in Hydrostatic Pressure and Pulse Transit Time to Measure Arterial Blood Pressure*. in *Engineering in Medicine and Biology Society, 2007. EMBS 2007. 29th Annual International Conference of the IEEE*. 2007.

92. C. C. Y. Poon, Y. T. Zhang, and Y. B. Liu. *Modeling of Pulse Transit Time under the Effects of Hydrostatic Pressure for Cuffless Blood Pressure Measurements*. in *the 3rd IEEE-EMBS International Summer School and Symposium on Medical Devices and Biosensors*. 2006. Boston, MA, USA.

93. M. Nitzan, et al., *Effects of external pressure on arteries distal to the cuff during sphygmomanometry*. IEEE Trans Biomed Eng., 2005. **52**: p. 1120-1127.

94. X. F. Teng and Y.T. Zhang, *The effect of applied sensor contact force on pulse transit time*. Physiol. Meas., 2006. **27**(8): p. 675–684.

95. Y. B. Liu, C. C. Y. Poon, and Y. T. Zhang. *The Changes in Pulse Transit Time at Specific Cuff Pressures during Inflation and Deflation*. in *EMBS '06. 28th Annual International Conference of the IEEE*. 2006. NYC, U. S.

96. W. W. Nichols and M.F. O'Rourke, *McDonald's Blood Flow in Arteries*. 5th ed. 2005, london: Arnold.

97. Y. S. Yan and Y. T. Zhang. *A Model-based calibration method for noninvasive and cuffless measurement of arterial blood pressure*. in *IEEE Biomedical Circuits and Systems Conf. 2006*. 2006. London.

98. A. J. Bank, et al., *In vivo human brachial artery elastic mechanics: effects of smooth muscle*

relaxation. Circulation, 1999. **100**(1): p. 41-47.

99. J. Gundersen, *Hydrostatic Changes of the Systolic Digital Blood Pressure.* Vasa., 1980. **9**(3): p. 197–200.
100. J. Y. Foo, et al., *Pulse transit time changes observed with different limb positions.* Physiol. Meas., 2005. **26**(6): p. 1093–1102.
101. Y. B. Liu and Y. T. Zhang. *Pulse Transit Time and Arterial Blood Pressure at Different Vertical Wrist Positions.* in *the International Special Topic Conference on Information Technology in Biomedicine*. 2006. Ioannina, Greece.
102. R. J. Vidmar, *Physiology and biophysics of the circulation.* 2nd ed. 1972, U.S.A: Year Book Medical Publishers, Inc.
103. B. Gribbin, A.S.A.a.P.S., *Pulse-wave velocity as a measure of blood-pressure change.* Psychophysiology, 1976. **13**(1): p. 86–90.
104. C. C. Y. Poon, Y. T. Zhang, and Y. B. Liu. *Modeling of Pulse Transit Time under the Effects of Hydrostatic Pressure for Cuffless Blood Pressure Measurements.* in *the 3rd IEEE-EMBS International Summer School and Symposium on Medical Devices and Biosensors.* 2006. Boston, MA, USA,.
105. P. Shaltis, A. Reisner, and H. Asada. *A hydrostatic pressure approach to cuffless blood pressure monitoring.* in *Proc. 26th Annu. Int. Conf. of IEEE Engineering in Medicine and Biology Society*. 2004. San Francisco, U.S.A.
106. R. A. Payne, et al., *Pulse transit time measured from the ECG: an unreliable marker of beat-to-beat blood pressure.* Appl Physiol, 2006. **100**: p. 136-141.
107. B. Gribbin, A. Steptoe, and P. Sleight, *Pulse-wave velocity as a measure of blood-pressure change.* Psychophysiology, 1976. **13**(1): p. 86–90.
108. C. C. Y. Poon, Y. T. Zhang, and Y. B. Liu. *Modeling of Pulse Transit Time under the Effects of Hydrostatic Pressure for Cuffless Blood Pressure Measurements.* in *the 3rd IEEE-EMBS International Summer School and Symposium on Medical Devices and Biosensors.* 2006. Boston, MA, USA,.
109. D. B. McCombie, A. T. Reisner, and H.H. Asada. *Motion Based Adaptive Calibration of Pulse Transit Time Measurements to Arterial Blood Pressure for an Autonomous, Wearable Blood Pressure Monitor.* in *30th Annual International IEEE EMBS Conference*. 2008. Vancouver, Canada.
110. D. B. Newlin, *Relationships ol Pulse Transmission Times to Pre-ejection Period and Blood Pressure.* Psychophysiology, 1980. **18**(3): p. 316-321.
111. D.Sujay, et al. *Cuff-Less Estimation of Blood Pressure Using Pulse Transit Time and Pre-ejection Period.* in *Convergence Information Technology, 2007. International Conference on*. 2007.
112. J. Allen and A. Murray, *Modelling the relationship between peripheral blood pressure and blood volume pulses using linear and neural network system identification techniques.* Physiological Measurement, 1999. **20**: p. 287-301.
113. S. C. Millasseau, et al., *Noninvasive Assessment of the Digital Volume Pulse : Comparison With the Peripheral Pressure Pulse*. 2000. p. 952-956.
114. L. Wang, E. Pickwell-MacPherson, and Y. T. Zhang. *Blood Pressure Contour Analysis after Exercise by the Photoplethysmogram Using a Transfer Function Method.* in *Proc. of the 5th International Workshop on Wearable and Implantable Bldy Sensor Networks*. 2008. Hong Kong.